

The Study on Signaling Mechanisms by Endogenous
N-Formylated Peptides

内因性 *N*-ホルミルペプチドによる情報伝達機構
に関する研究

Doctoral Thesis

Submitted to Graduate School of Bioscience

Nagahama Institute of Bio-Science and Technology

Takayuki Marutani

September 2021

TABLE OF CONTENTS

Contents	• • • • •	1
Abbreviations	• • • • •	3
<u>Chapter I</u>	General Introduction • • • • •	5
<u>Chapter II</u>	Mitocryptide-2: Identification of Its Minimum Structure for Specific Activation of FPR2–Possible Receptor Switching from FPR2 to FPR1 by Its Physiological C-terminal Cleavages • • • • •	12
II-1. Abstract	• • • • •	13
II-2. Introduction	• • • • •	14
II-3. Materials and Methods	• • • • •	16
II-4. Results	• • • • •	25
II-5. Discussion	• • • • •	41
<u>Chapter III</u>	Physiological Existence of Endogenous N-Formylated Peptides • •	53
III-1. Abstract	• • • • •	54
III-2. Introduction	• • • • •	55
III-3. Materials and Methods	• • • • •	56

Abbreviations

Ala: L-Alanine

Arg: L-Arginine

Cys: L-Cysteine

Gly: Glycine

Ile: L-Isoleucine

Lys: L-Lysine

Phe: L-Phenylalanine

Ser: L-Serine

Trp: L-Tryptophan

Val: L-Valine

Asn: L-Asparagine

Asp: L-Aspartic acid

Glu: L-Glutamic acid

His: L-Histidine

Leu: L-Leucine

Met: L-Methionine

Pro: L-Proline

Thr: L-Threonine

Tyr: L-Tyrosine

ATP6: ATP synthase subunit protein 6

ATP8: ATP synthase subunit protein 8

$[Ca^{2+}]_i$: Concentration of intracellular free Ca^{2+}

CD: Circular dichroic

COX1: Cytochrome *c* oxidase subunit I

COX2: Cytochrome *c* oxidase subunit II

COX3: Cytochrome *c* oxidase subunit III

CysH: Cyclosporin H

EC₅₀: Effective concentration

EM: Electron microscopy

fMLF: Formyl-Met-Leu-Phe

FPR1: Formyl peptide receptor 1

FPR2: Formyl peptide receptor 2

HBHS: HEPES-buffered Hank's solution

IL-8: Interleukin 8

MS: Mass spectrometry

MCT-CYC: Mitocryptide-CYC

MCT-1: Mitocryptide-1

MCT-2: Mitocryptide-2

mtDNA: Mitochondrial DNA

mtDAMPs: Mitochondrial damage-associated molecular patterns

ND1: NADH dehydrogenase subunit 1

ND2: NADH dehydrogenase subunit 2

ND3: NADH dehydrogenase subunit 3

ND4L: NADH dehydrogenase subunit 4L

ND4: NADH dehydrogenase subunit 4

ND5: NADH dehydrogenase subunit 5

ND6: NADH dehydrogenase subunit 6

RP: Reverse phase

TFE: 2,2,2-trifluoroethanol

Chapter I
General Introduction

Neutrophils are a type of leukocytes that are involved in the innate defense system [1–3]. Neutrophils comprise the majority of peripheral leukocytes and normally exist in bloodstream to monitor for infection and tissue damage. When tissue injury occurs due to bacterial infections or internal tissue damage, neutrophils immediately migrate to and infiltrate injury sites. Infiltrated neutrophils are then activated and exert their functions including superoxide production and phagocytosis of invading bacterial components and toxic substances.

Bacterial *N*-formylated proteins and peptides are well known as chemoattractants for neutrophils. In 1975, Schiffmann *et al.* found that bacterial *N*-formylated proteins and peptides induced neutrophil migration and activation [4]. Subsequently, various bacterial *N*-formylated peptides including formyl-Met-Leu-Phe (fMLF) were identified from bacterial culture supernatants as chemoattractants for neutrophils [5, 6]. Moreover, Carp demonstrated that endogenous *N*-formylated proteins or peptides in mitochondria possibly induce migration of neutrophils [7], although such neutrophil-migrating *N*-formylated proteins and peptides have not been molecularly identified.

In addition to such *N*-formylated proteins and peptides, complement-derived factors have been also identified as chemoattractants for neutrophils [8, 9]. Indeed, several complement proteins are cleaved by complement system, and various fragment peptides are produced during activation of the complement system by invading microbes. Among those fragments, component 3a and 5a have been found to chemoattract neutrophils to promote inflammatory reactions [8, 9]. Moreover, it has been shown that some CXC chemokines such as IL-8 promote migration and activation

of neutrophils [10, 11]. Specifically, these CXC chemokines are translated and produced in damaged tissues behind the initial migration of neutrophils [12]. These chemokines induce "delayed" dramatic infiltration and activation of neutrophils to promote inflammation.

In this way, various neutrophil-activating factors consisting of bacterial *N*-formylated peptides, complement-derived factors, and CXC chemokines have been identified. However, these factors might not be the substances to promote the initial migration and activation of neutrophils. Namely, immediate neutrophil migration into damaged tissues is observed even in non-infectious tissue injury such as ischemia reperfusion injury, trauma and burn. Moreover, it is believed that CXC chemokines unable to induce initial infiltration of neutrophils because they are produced translationally in injury tissues behind the initial migration of neutrophils [12]. In addition, it is controversial whether complement-derived peptides induce neutrophil migration by forming a concentration gradient from injury tissues, because complement-derived factors are mainly located in bloodstream. Hence, it had been unclear what substances induce initial neutrophil migration and activation.

Mukai and his colleagues therefore attempted to purify such neutrophil-activating factors from healthy porcine heart, because immediate and dramatic infiltration of neutrophils after ischemia reperfusion injury in the heart causes severe tissue damage. They successfully isolated and identified three novel neutrophil-activating peptides mitocryptide-1 (MCT-1), mitocryptide-2 (MCT-2), and mitocryptide-CYC (MCT-CYC),

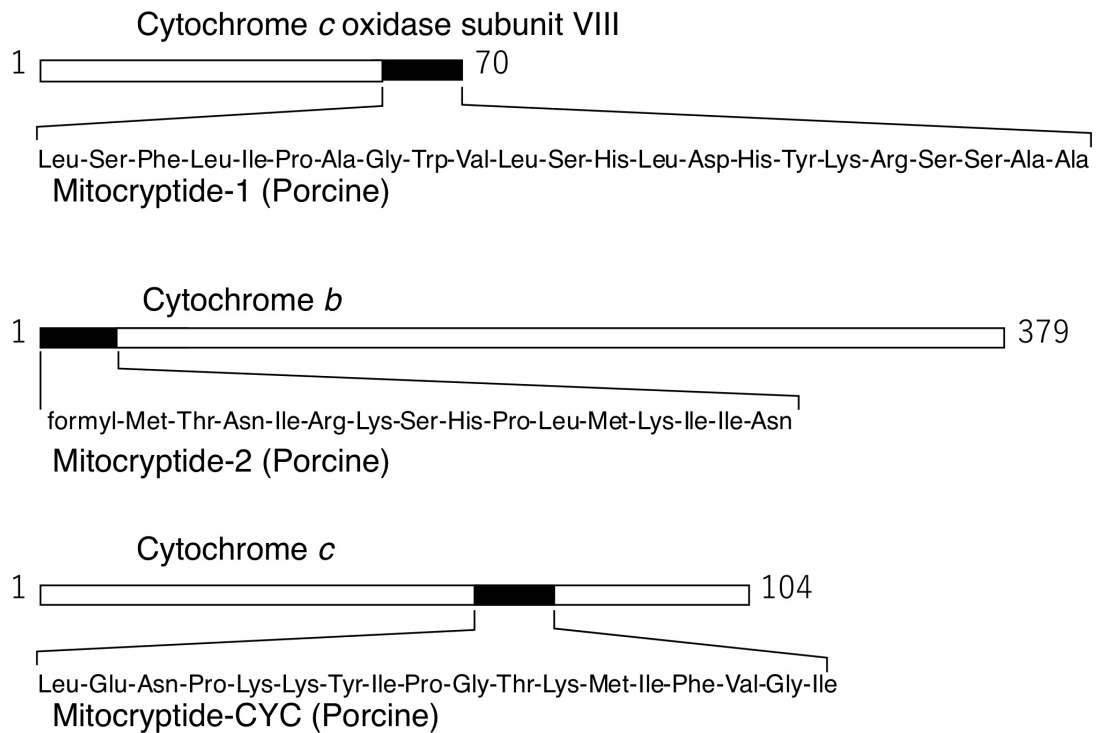


Figure I-1. Primary structures of MCT-1, MCT-2, and MCT-CYC, and their positions in the parent proteins.

which are derived from mitochondrial cytochrome *c* oxidase subunit VIII, cytochrome *b*, and cytochrome *c*, respectively (Figure I-1) [13-15]. They also found the presence of many fractions that induced neutrophilic activation other than those containing MCT-1, MCT-2, and MCT-CYC, and tried to determine the chemical structures of these peptidergic substances in those fractions. Although their complete structures are not yet determined, most of those peptides were shown to be fragments of various mitochondrial proteins. These observations suggest that neutrophils are regulated by many peptides derived from mitochondrial proteins. They therefore named such functional cryptic peptides that are hidden in protein structures as “cryptides”, and those cryptides that are derived from mitochondrial proteins as “mitocryptides”[16].

After the discovery of mitocryptides, it has been accumulating the evidence that indicates the involvement of mitochondria and their derived substances in innate immunity. Indeed, various tissues damaged by trauma or burn release mitochondria and their contents into bloodstream [17-23]. They are also released from a variety of cells damaged by bacterial infection [23-27]. In addition, it is suggested that they are leaked into the cerebrospinal fluid from damaged tissues in patients with Alzheimer’s disease [28, 29]. These released mitochondria and their derived factors, which are called mitochondrial damage-associated molecular patterns (mtDAMPs), promote various innate immune responses including induction of neutrophil and macrophage migration and activation [17, 19, 23, 30, 31]. MtDAMPs also stimulate the secretion of inflammatory mediators from mast cells [32].

However, it is still unclear what factors in mtDAMPs induce innate immune

responses. Namely, mitochondrial DNA (mtDNA) and *N*-formylated peptides and proteins are believed to be activating factors in mtDAMPs. Indeed, it has been shown that levels of mtDNA released into the circulation in trauma patients were markedly elevated in comparison with healthy volunteers, and the released mtDNA may induce sterile inflammation [17]. However, highly purified mtDNA was recently demonstrated to be unable to induce neutrophilic responses, thus neutrophilic activation by mtDNA is still controversial [33]. On the other hand, although inhibitors against the functions of *N*-formylated peptides partially inhibit the abilities of mtDAMPs [17, 19, 30], endogenous *N*-formylated peptides in mtDAMPs have not been identified yet. Since MCT-2 is the only endogenous *N*-formylated peptide that has been isolated from mammalian tissues and its complete chemical structure has been determined, it is a leading candidate for activating factors in mtDAMPs.

As receptors for such *N*-formylated proteins and peptides including bacterial ones as well as MCT-2, formyl peptide receptor 1 (FPR1, formerly referred to as formyl peptide receptor) and formyl peptide receptor 2 (FPR2, formerly referred to as formyl peptide receptor-like 1) are known to be expressed on the cell membrane of neutrophils [34-39]. MCT-2 specifically binds to and activates FPR2, but it neither interacts with nor activates FPR1, indicating that MCT-2 is an endogenous specific ligand for FPR2 [37]. However, the recognition mechanisms of MCT-2 by FPR2 remain unclear.

In the present study, I therefore investigated the structure–activity relationships of MCT-2 and its derivatives to elucidate how FPR2 specifically recognizes MCT-2, and showed that the *N*-terminal heptapeptide structure of MCT-2 with an *N*-formyl group

was the minimum structure that was specifically recognized by FPR2 for its activation. Moreover, the receptor for MCT-2 was surprisingly demonstrated to be shifted from FPR2 to its homologue FPR1 depending on alterations of its molecular forms, suggesting that MCT-2 is a factor that controls not only the initiation of innate immune responses against tissue injury but also different responses via the activation of FPR1, which may related to resolution and wound healing/tissue regeneration (Chapter II).

Although MCT-2 was considered to be a first-line candidate as a peptidergic activating factor in mtDAMPs, is it the only endogenous *N*-formylated peptide? It is possible that endogenous *N*-formylated peptides other than MCT-2 are produced and activate FPR1 and/or FPR2 to induce innate immune responses including neutrophil infiltration and activation, since thirteen proteins are encoded in mitochondrial DNA and are translated in mitochondria as *N*-formylated forms [40, 41]. Thus, I also examined the possible existence of endogenous *N*-formylated peptides other than MCT-2 for the induction of innate immune responses. Here I show that several putative *N*-formylated peptides derived from mtDNA-encoded proteins had potencies comparable to or higher than MCT-2 in the activation of neutrophilic cells, suggesting that endogenous *N*-formylated peptides other than MCT-2 may also regulate innate immune responses (Chapter III). Based on the evidence described in Chapters II and III, the innate immune mechanisms involving endogenous *N*-formylated peptides was discussed in Chapter IV.

Chapter II

Mitocryptide-2: Identification of Its Minimum

Structure for Specific Activation of FPR2

**–Possible Receptor Switching from FPR2 to
FPR1 by Its Physiological C-terminal Cleavage**

II-1. Abstract

Mitocryptides are a novel family of endogenous neutrophil-activating peptides originated from various mitochondrial proteins. Mitocryptide-2 (MCT-2) is one of such neutrophil-activating peptides and is produced as an *N*-formylated pentadecapeptide from mitochondrial cytochrome *b*. Although MCT-2 is a specific endogenous ligand for formyl-peptide receptor 2 (FPR2), the chemical structure within MCT-2 that is responsible for FPR2 activation is still obscure. Here, I demonstrate that the *N*-terminal heptapeptide structure of MCT-2 with an *N*-formyl group is the minimum structure that specifically activates FPR2. Moreover, the receptor molecule for MCT-2 is suggested to be shifted from FPR2 to its homolog formyl-peptide receptor 1 (FPR1) by the physiological cleavages of its *C*-terminus. Indeed, *N*-terminal derivatives of MCT-2 with 7 amino acid residues or longer than it caused an increase of intracellular free Ca^{2+} concentration in HEK-293 cells expressing FPR2 but not in those expressing FPR1. Those MCT-2 derivatives also induced β -hexosaminidase secretion in neutrophilic/granulocytic differentiated HL-60 cells via FPR2 activation. In contrast, MCT-2(1–4), an *N*-terminal tetrapeptide of MCT-2, specifically activated FPR1 to promote those functions. Moreover, MCT-2 was degraded in serum to produce MCT-2(1–4) over time, suggesting that the receptor for MCT-2 was shifted from FPR2 to FPR1 by its *C*-terminal cleavage. These findings suggest that MCT-2 is a novel critical factor that initiates not only innate immunity via the specific activation of FPR2 but also promotes delayed responses by the activation of FPR1 which may include resolution and tissue regeneration.

II-2. Introduction

Most peptides present in mammals are produced by proteolytic cleavage of precursor proteins. That is, functional proteins are first synthesized as precursor proteins, which are then cleaved by various processing enzymes to produce mature bioactive proteins. After playing their physiological roles, they are inactivated by various proteases. During maturation and degradation of these functional proteins, many peptide fragments are simultaneously produced. For a long time, these peptide fragments were thought to be metabolites without physiological functions.

However, Mukai and his colleagues found that some of these peptides efficiently induce innate immune responses including neutrophil activation. Namely, they have identified a novel family of neutrophil-activating peptides including MCT-1, MCT-2, and MCT-CYC that endogenously produced from various mitochondrial proteins [13-15]. Among them, MCT-2 is an *N*-formylated pentadecapeptide derived from mitochondrial cytochrome *b* and is found to promote neutrophilic migration and phagocytosis efficiently. Signaling mechanisms of neutrophil activation by MCT-2 have been investigated at the cellular level, and MCT-2 has been demonstrated to be an endogenous specific ligand for FPR2 [37]. In addition, MCT-2 was shown to induce neutrophilic functions as a result of G_{12} -protein-dependent intracellular signaling events including $[Ca^{2+}]_i$ increase and ERK1/2 phosphorylation [14, 37]. However, the chemical structure within MCT-2 that is specifically recognized by FPR2 is unclear.

In this chapter, I investigated the structure–activity relationships of MCT-2 and its derivatives to elucidate how FPR2 recognizes MCT-2. I also explored the

time-dependent alterations of the molecular forms of MCT-2 in serum and attempted to elucidate the meaning of these alterations in innate immune responses.

II-3. Materials and Methods

II-3-1. Peptide synthesis

Human MCT-2 and its derivatives were chemically synthesized by a solid-phase method [42-45] using a 9-fluorenylmethyloxycarbonyl strategy [14, 37]. Synthetic peptides were purified by reverse phase (RP)-HPLC on a 5C₁₈ column (20 × 250 mm, COS-MOSIL; Nacalai Tesque, Inc., Kyoto, Japan). These peptides were analyzed by RP-HPLC on a 5C₁₈ column (4.6 × 150 mm, COSMOSIL; Nacalai Tesque, Inc.) and were proven to be more than 95% pure (Figure II-1,II-2). The molecular weights of the synthesized peptides were also confirmed by MALDI-TOF-mass spectrometry (MS) (Table II-1). fMLF was purchased from Nacalai Tesque, Inc.

II-3-2. Preparation of cells

HEK-293 cells (American Type Culture Collection, Manassas, VA, USA) were maintained in DMEM (Thermo Fisher Scientific, Waltham, MA, USA) containing 10% FBS (Thermo Fisher Scientific) in a humidified atmosphere at 5% CO₂ and 37°C. Human acute leukemia-derived HL-60 cells (RIKEN Cell Bank, Ibaraki, Japan) were cultured in RPMI-1640 medium (Thermo Fisher Scientific) containing 10% FBS in a humidified atmosphere at 5% CO₂ and 37 °C. HL-60 cells were treated with 500 μM dibutyryl-cAMP (Sigma-Aldrich, St. Louis, MO) for 72 h to differentiate the cells into neutrophilic/granulocytic cells as described elsewhere [13-15, 37, 46].

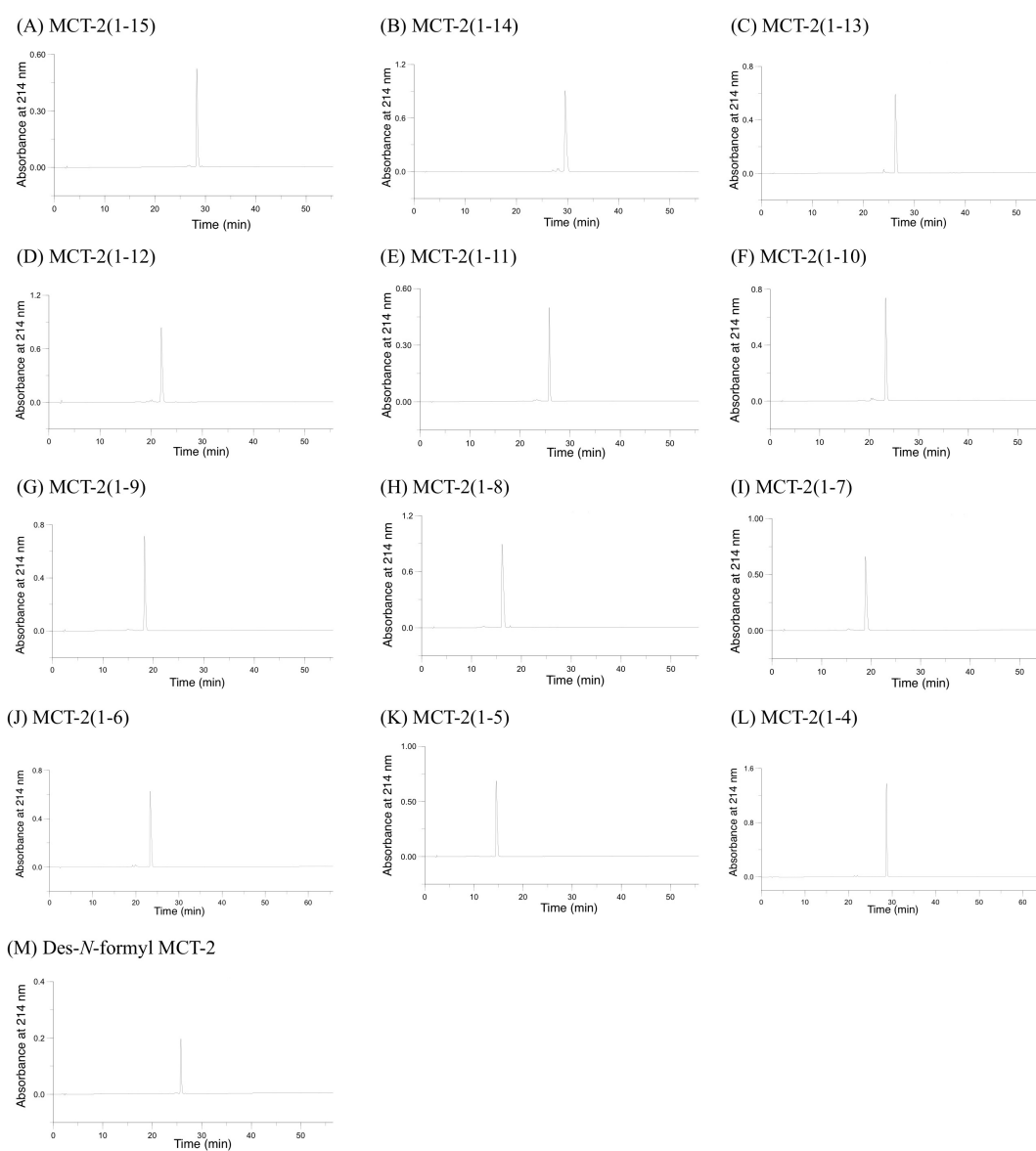


Figure II-1. Analytical RP-HPLC profiles of MCT-2(1–15) (A), MCT-2(1–14) (B), MCT-2(1–13) (C), MCT-2(1–12) (D), MCT-2(1–11) (E), MCT-2(1–10) (F), MCT-2(1–9) (G), MCT-2(1–8) (H), MCT-2(1–7) (I), MCT-2(1–6) (J), MCT-2(1–5) (K), MCT-2(1–4) (L), and Des-*N*-formyl MCT-2 (M). Analytical conditions: column, 5C₁₈ column (4.6 × 150 mm); elution with a linear gradient from 10% to 60% CH₃CN/0.1% trifluoroacetic acid for 50 min (A–I, K and M) or 0% to 60% CH₃CN/0.1% trifluoroacetic acid for 60 min (J and L); flow rate, 1 mL/min; detection wavelength, 214 nm.

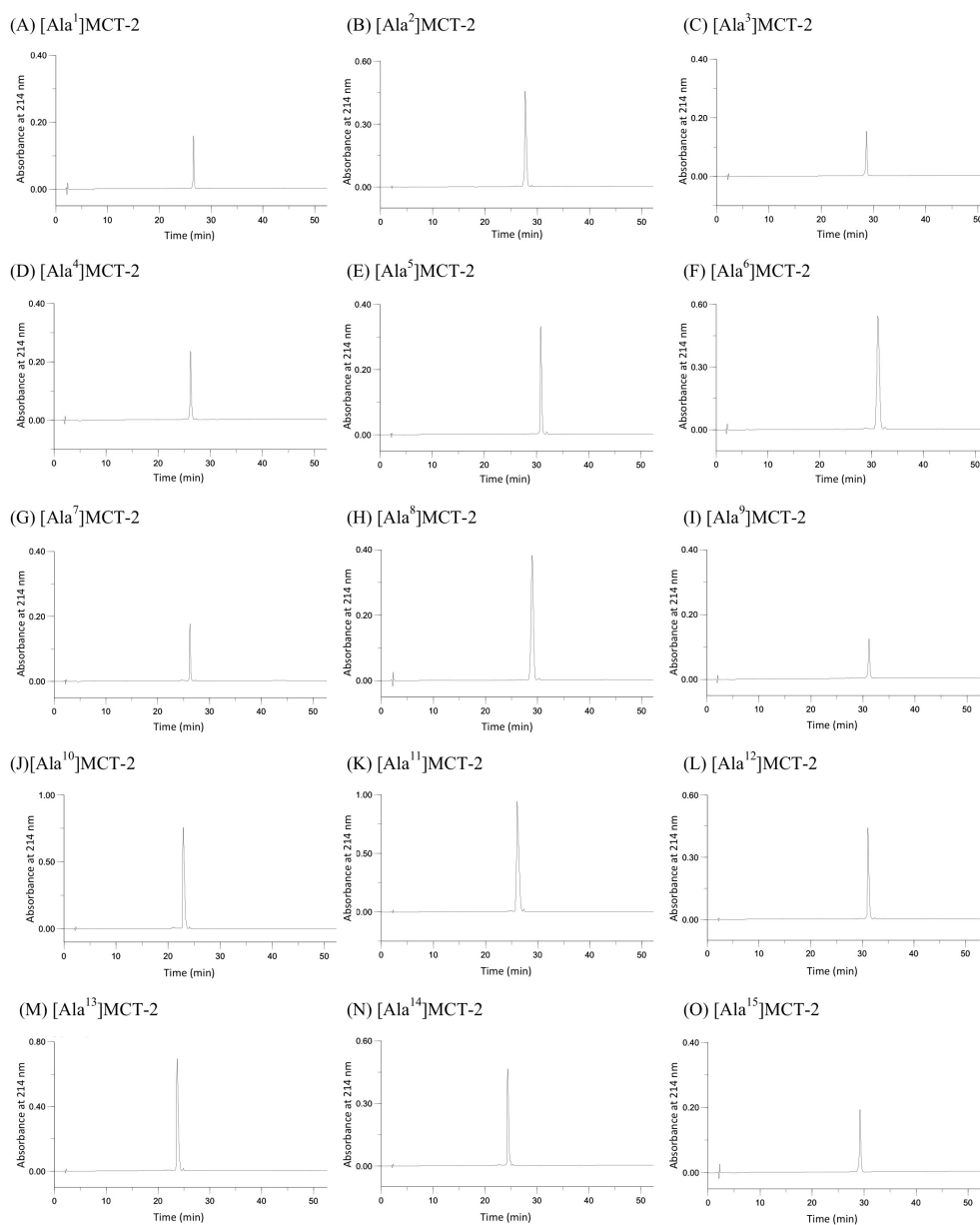


Figure II-2. Analytical RP-HPLC profiles of [Ala¹]MCT-2 (A), [Ala²]MCT-2 (B), [Ala³]MCT-2 (C), [Ala⁴]MCT-2 (D), [Ala⁵]MCT-2 (E), [Ala⁶]MCT-2 (F), [Ala⁷]MCT-2 (G), [Ala⁸]MCT-2 (H), [Ala⁹]MCT-2 (I), [Ala¹⁰]MCT-2 (J), [Ala¹¹]MCT-2 (K), [Ala¹²]MCT-2 (L), [Ala¹³]MCT-2 (M), [Ala¹⁴]MCT-2 (N), and [Ala¹⁵]MCT-2 (O). Analytical conditions: column, 5C₁₈ column (4.6 × 150 mm); elution with a linear gradient from 10% to 60% CH₃CN/0.1% trifluoroacetic acid for 50 min; flow rate, 1 mL/min; detection wavelength, 214 nm.

Table II-1. Analytical data by MALDI-TOF-MS for MCT-2(1–15) and its derivatives.

Peptide	MALDI-TOF-MS (m/z, [M+H] ⁺)	
	Observed	Calculated
MCT-2(1-15)	1827.81	1828.03
MCT-2(1-14)	1713.61	1713.98
MCT-2(1-13)	1600.88	1600.88
MCT-2(1-12)	1487.7	1487.79
MCT-2(1-11)	1359.69	1359.72
MCT-2(1-10)	1228.60	1228.70
MCT-2(1-9)	1115.55	1115.58
MCT-2(1-8)	1018.56	1018.52
MCT-2(1-7)	904.42	904.49
MCT-2(1-6)	791.36	791.40
MCT-2(1-5)	663.35	663.31
MCT-2(1-4)	529.19 ^a	507.21
Des- <i>N</i> -formyl MCT-2	1799.99	1800.01
[Ala ¹]MCT-2	1769.27	1769.20
[Ala ²]MCT-2	1799.75	1799.29
[Ala ³]MCT-2	1803.24	1803.28
[Ala ⁴]MCT-2	1769.21	1769.21
[Ala ⁵]MCT-2	1743.97	1744.21
[Ala ⁶]MCT-2	1772.75	1772.22
[Ala ⁷]MCT-2	1787.51	1787.24
[Ala ⁸]MCT-2	1786.55	1786.29
[Ala ⁹]MCT-2	1803.38	1803.28
[Ala ¹⁰]MCT-2	1787.36	1787.24
[Ala ¹¹]MCT-2	1769.47	1769.21
[Ala ¹²]MCT-2	1772.35	1772.22
[Ala ¹³]MCT-2	1787.60	1787.24
[Ala ¹⁴]MCT-2	1787.81	1787.24
[Ala ¹⁵]MCT-2	1786.98	1786.29

^aSignal corresponding to a sodiated peptide ([M+Na]⁺).

II-3-3. Establishment of HEK-293 cells stably expressing FPR1 or FPR2

HEK-293 cells stably expressing FPR1 or FPR2 with a $G\alpha_{16}$ type of G protein were established, as described previously [37]. Briefly, HEK-293 cells were transfected with human FPR1/pcDNA3.1/Zeo or human FPR2/pcDNA3.1/Zeo using Lipofectamine 2000 (Thermo Fisher Scientific). The cells were also co-transfected with $G\alpha_{16}$ /pcDNA3.1/Hygro to induce an agonist-promoted increase in $[Ca^{2+}]_i$. One cell was placed into each well of a 96-well plate and selected with 100 $\mu\text{g}/\text{mL}$ hygromycin (FUJIFILM Wako Pure Chemical, Osaka, Japan) and 250 $\mu\text{g}/\text{mL}$ Zeocin (InvivoGen, San Diego, CA, USA). Individual cells were further selected by measuring increases in $[Ca^{2+}]_i$ stimulated by 1 μM fMLF.

II-3-4. Measurement of $[Ca^{2+}]_i$

The increase in $[Ca^{2+}]_i$ stimulated by peptides was assessed, as described previously [13, 37]. In brief, HEK-293 cells stably expressing FPR1 or FPR2 with a $G\alpha_{16}$ type of G protein were washed twice with a HEPES–Na solution (5 mM HEPES, 140 mM NaCl, 4 mM KCl, 1 mM NaH_2PO_4 , 1 mM MgCl_2 , 1.25 mM CaCl_2 , 11 mM glucose, and 0.2% BSA, pH 7.4). The Ca^{2+} -sensitive fluorescence reagent Fura-2-acetoxymethyl ester (Dojin, Kumamoto, Japan) was added to the cell suspension (4 mL; final concentration: 4 μM). The reaction mixture was shielded from light and shaken gently at 37 °C for 60 min to load the cells with Fura-2. The cells were subsequently washed twice with the HEPES–Na solution and a cell suspension was

diluted to a final density of 5.0×10^5 cells/mL. The cell suspension (1 mL) was placed into a cuvette and stimulated by peptide solutions (5 μ L) with stirring at 37 °C. The ratio of fluorescence intensity at 500 nm by excitation wavelengths of 340 nm and 380 nm was measured using a fluorometer (CAF-100; Japan Spectroscopic Co., Tokyo, Japan).

II-3-5. Assay of β -hexosaminidase release

The ability of MCT-2-related peptides to activate HL-60 cells differentiated into neutrophilic/granulocytic cells was evaluated by stimulation of β -hexosaminidase secretion from the cells [13-15, 47]. Briefly, differentiated HL-60 cells were washed 3 times with ice-cold HEPES-buffered Hank's solution (HBHS; 10 mM HEPES, 136.9 mM NaCl, 5.4 mM KCl, 1.2 mM CaCl₂, 0.44 mM KH₂PO₄, 0.49 mM MgCl₂, 0.41 mM MgSO₄, 0.34 mM Na₂HPO₄, 5.5 mM glucose, 4.2 mM NaHCO₃, and 0.1% BSA, pH 7.4). The cells were resuspended in HBHS at a density of 5.6×10^6 cells/mL, and DNase I (Sigma-Aldrich) and cytochalasin B (Sigma-Aldrich) were each added at a final concentration of 5 μ g/mL. The cell suspension in each tube (5.0×10^5 cells/ 90 μ L) was preincubated at 37 °C for 10 min and stimulated with 10 μ L synthetic peptide solution at 37 °C for 10 min. The inhibitory effects of inhibitors against FPR1 [cyclosporin H (CysH)] (Sigma-Aldrich) and FPR2 [PBP10 (Tocris Bio-science, Bristol, UK)] on β -hexosaminidase release induced by MCT-2 and its derivatives were also evaluated in the differentiated HL-60 cells; each cell suspension prepared as above (90 μ L) was transferred to a tube (5.0×10^5 cells/tube) with 5 μ L inhibitor solution for

FPR1 (CysH) or FPR2 (PBP10). Each tube was then preincubated at 37 °C for 10 min and stimulated with 5 µL synthetic peptide solution at 37 °C for 10 min. After stimulation, 200 µL ice-cold reaction quenching buffer (25 mM Tris, 123 mM NaCl, and 2.7 mM KCl, pH 7.4) was added to each cell suspension to stop the reaction. Thereafter, these tubes were centrifuged at 4 °C and 2300 × g for 1 min, and each supernatant was transferred into a new tube.

β-Hexosaminidase activity in the supernatant was measured as described previously [47]. Briefly, 90 µL supernatant was transferred to each well of a 96-well microtiter plate, and 60 µL of a substrate solution for β-hexosaminidase [10 mM p-nitrophenyl *N*-acetyl-β-D-glucosaminide (Sigma-Aldrich), 40 mM citrate, and 70 mM NaHPO₄, pH 4.5] was added to initiate the enzyme reaction. After incubation of the plate at 37 °C for 1 h, 100 µL of 400 mM glycine (pH 10.7) was added to stop the reaction. The absorbance at 415 nm for the resulting p-nitrophenol and at 490 nm for the reference was measured using a microtiter plate reader (Viento XS; BioTek Instruments, Winooski, VT, USA).

The ability of each peptide to induce β-hexosaminidase release was expressed as a percentage of enzyme secretion promoted by 10 µM MCT-2(1–15) that induced the maximum response for the elucidation of full or partial agonists to the activity of MCT-2(1–15) (Figures II-4 and II-6, Table II-2) or a percentage of the total enzyme activity, which was the enzyme activity released after disruption of the cells with 0.05% Triton X-100 (Figure II-5).

II-3-6. Measurement of circular dichroic spectra

Circular dichroic (CD) spectra of the synthetic peptides were obtained at 25 °C using a J-820 spectrometer (Jasco, Tokyo, Japan) in a quartz cell with a 0.1 cm path length. Spectra were collected between 190 nm and 250 nm with a scan speed of 50 nm/min, response time of 1 s, and bandwidth of 1 nm. Peptide samples with a final concentration of 100 µM were prepared in 10 mM phosphate buffer (pH 7.4) containing 0% or 50% TFE. The baseline scan, which was acquired by measuring the buffer alone, was subtracted from the experimental readings. CD data, which were collected every 1 nm, were the average of 5 scans. The results were expressed as the optical rotation (mdeg).

II-3-7. Analysis of time-dependent alterations of MCT-2 molecular forms in serum

The animal experiments were conducted under the guidance of the Animal Care and Use Committee of the Nagahama Institute of Bio-Science and Technology (Approved No. 047). C57BL/6JJcl mice were purchased from Clea Japan (Tokyo, Japan). All mice were maintained in the Animal Research Facility at the Nagahama Institute of Bio-Science and Technology.

Male C57BL/6JJcl mice, 12–14 weeks of age, weighing 25–30 g, were anesthetized (50 mg/kg pentobarbital), and blood was collected from the caudal vena cava and stored overnight at 4 °C. The blood sample was centrifuged at 4 °C and 20,000 × g for 20 min, and the supernatant was transferred to a new tube as mouse serum and stored at –80 °C. MCT-2 was incubated in mouse serum at a final concentration of 500

μM at $37\text{ }^{\circ}\text{C}$, and aliquots ($100\text{ }\mu\text{L}$) were collected from the incubation mixture after 0, 1, 2, 4, 24, and 48 h. These aliquots were mixed with TCA (final concentration: 3% w/v) and kept on ice for 30 min to precipitate denatured proteins. The samples were centrifuged at $4\text{ }^{\circ}\text{C}$ and $13,000 \times g$ for 15 min, and the supernatants were analyzed by RP-HPLC on a 5C_{18} column ($4.6 \times 150\text{ mm}$, Cosmosil; Nacalai Tesque, Inc.). RP-HPLC peaks that contained MCT-2 and its derivative peptides were analyzed by MALDI-TOF-MS to identify their molecular forms.

II-3-8. Statistical Analysis

Data are expressed as the mean \pm standard error (SE) in experiments containing multiple data points. Statistical comparisons between two groups were performed using Student's t-test, and values of $p < 0.05$ were considered significant.

II-4. Results

II-4-1. Effects of MCT-2(1–15) and its derivatives on $[Ca^{2+}]_i$ in HEK-293 cells stably expressing FPR1 or FPR2

An endogenous pentadecapeptide, MCT-2 [MCT-2(1–15)], specifically binds to and activates FPR2, but it neither interacts with nor activates FPR1 [37]. In addition, MCT-2(1–10) or *N*-terminal derivatives longer than it specifically activate FPR2 to cause β -arrestin recruitment and superoxide production [48]. However, the precise structure within MCT-2(1–15) that is responsible for the specific activation of FPR2 is not known. Here, increases in the concentration of intracellular free Ca^{2+} ($[Ca^{2+}]_i$) promoted by MCT-2(1–15) and its derivatives were assessed in HEK-293 cells stably expressing FPR1 or FPR2 (Figure II-3). The $G\alpha_{16}$ type of G protein was also stably co-expressed in these cells because this protein interacts with various G protein-coupled receptors and effectively induces an agonist-promoted increase of $[Ca^{2+}]_i$ [49]. As a result, 100 μ M MCT-2(1–10), MCT-2(1–9), MCT-2(1–8), and MCT-2(1–7) as well as 10 μ M MCT-2(1–15) induced an increase of $[Ca^{2+}]_i$ in HEK-293 cells expressing FPR2, but not in FPR1-expressing cells (Figure II-3A–E). In contrast, 100 μ M MCT-2(1–5) induced an increase of $[Ca^{2+}]_i$ in FPR1- and FPR2-expressing cells (Figure II-3F). Moreover, 100 μ M MCT-2(1–4) promoted an increase of $[Ca^{2+}]_i$ in FPR1-expressing cells, but not in FPR2-expressing cells (Figure II-3G). In addition, stimulation with MCT-2(1–6) did not induce an increase of $[Ca^{2+}]_i$ in FPR2- or FPR1-expressing cells, even at a concentration of 100 μ M (data not shown). These results demonstrate that the

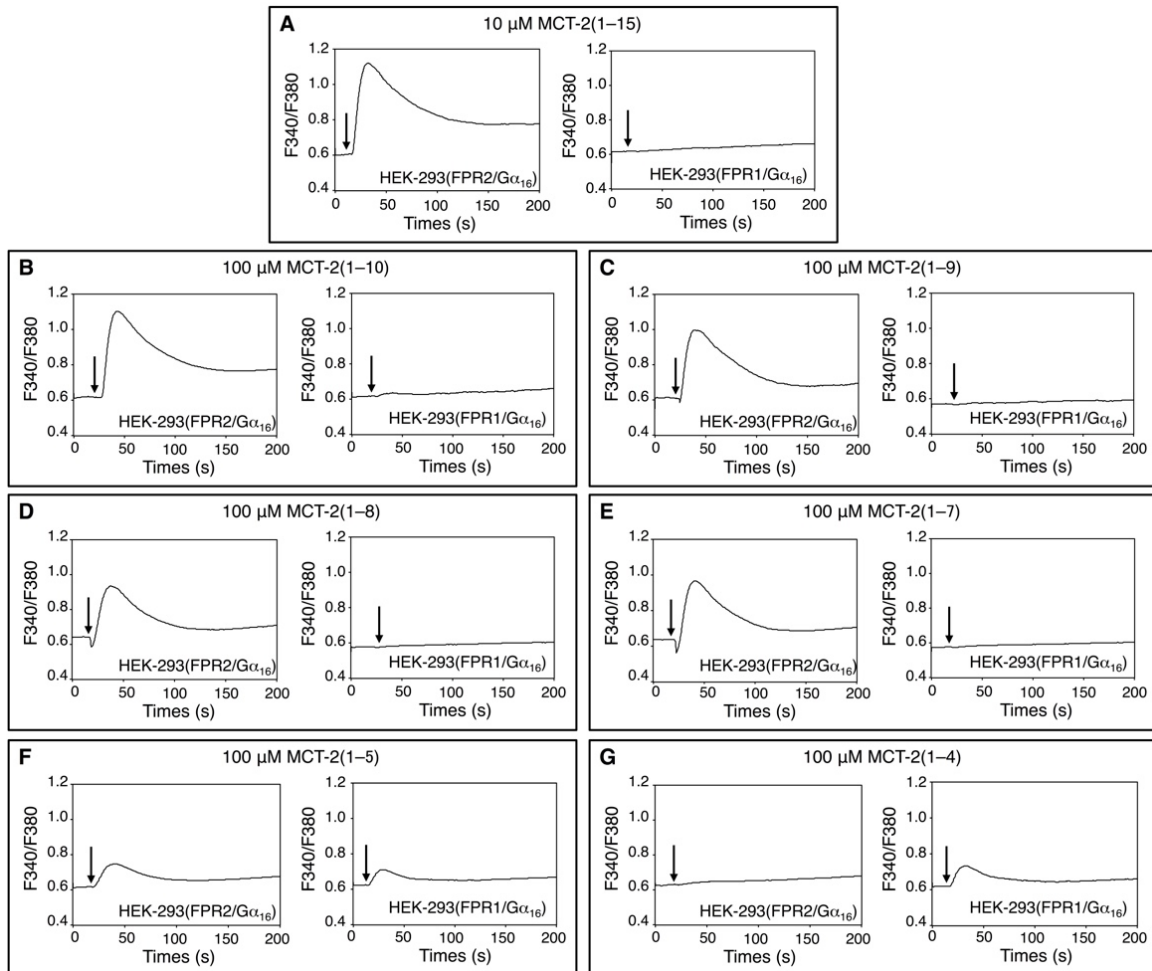


Figure II-3. Changes in $[Ca^{2+}]_i$ in HEK-293 cells stably expressing FPR1 (formyl peptide receptor 1) or FPR2 (formyl peptide receptor 2) induced by MCT-2 (Mitocryptide-2)(1-15) and its derivatives. Fura-2-loaded cells were stimulated with 10 μ M MCT-2(1-15) (A) or 100 μ M MCT-2(1-10) (B), MCT-2(1-9) (C), MCT-2(1-8) (D), MCT-2(1-7) (E), MCT-2(1-5) (F), and MCT-2(1-4) (G). The changes in the fluorescence ratio of Fura-2 (excitation wavelengths, 340 nm and 380 nm; emission wavelength, 500 nm) were recorded by a fluorometer CAF-100. Horizontal axes show the times after stimulation. Vertical axes depict the fluorescence ratios at excitation wavelengths of 340 nm and 380 nm. Arrows indicate the timing of peptide administration.

N-terminal derivative MCT-2(1–7) and its longer derivatives specifically activate FPR2, in contrast with MCT-2(1–4), which specifically activates FPR1.

II-4-2. Effects of C- or N-terminal truncations of MCT-2(1–15) on β -hexosaminidase release from neutrophilic/granulocytic differentiated HL-60 Cells

The effects of *N*- or *C*-terminal truncations of MCT-2 on β -hexosaminidase released from neutrophilic/granulocytic differentiated HL-60 cells were investigated to elucidate the minimum structure that was required for the activation of their receptor molecules. As our research group reported previously [14], a pentadecapeptide MCT-2 [MCT-2(1–15)] dose-dependently promoted β -hexosaminidase secretion from differentiated HL-60 cells (EC_{50} : 20 ± 3 nM, Figure II-4 and Table II-2), and the maximum response was observed at concentrations greater than 1 μ M.

To elucidate the necessity of the *N*-formyl group for this stimulation, I examined the effects of its removal from MCT-2(1–15). Des-*N*-formyl MCT-2(1–15) did not induce β -hexosaminidase release, even at a concentration of 100 μ M (Figure II-4A), demonstrating that the formyl group at the *N*-terminus of MCT-2(1–15) is crucial for this process.

Next, I examined the importance of the *C*-terminal sequence of MCT-2(1–15) for the stimulation of β -hexosaminidase release from differentiated HL-60 cells by performing *C*-terminal truncations. Truncations of one to eight amino acid residues

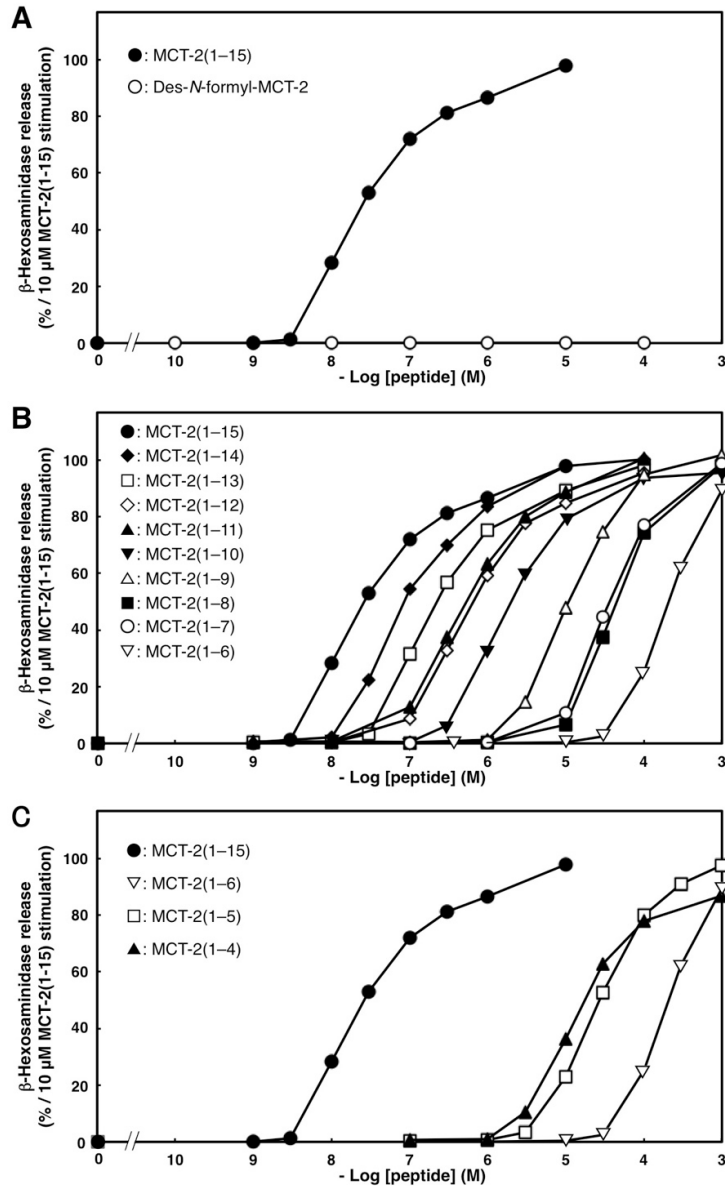


Figure II-4. Effects of *N*- or *C*-terminal truncations of MCT-2(1-15) on β -hexosaminidase release by differentiated HL-60 cells. The differentiated HL-60 cells were stimulated by MCT-2(1-15) or its derivatives at 37 °C for 10 min, and the amount of the released β -hexosaminidase was quantified as described in “Materials and Methods”. The ability of each peptide to induce β -hexosaminidase release is expressed as a percentage of enzyme secretion promoted by 10 μ M MCT-2(1-15). Data are expressed as the mean \pm SE of four to six independent experiments.

Table II-2. Amino acid sequences and experimental data for MCT-2(1–15) and its derivatives and their EC₅₀ values and maximum effects on the induction of β-hexosaminidase release from differentiated HL-60 cells.

Peptide	Sequence	EC ₅₀ (nM)	Maximum effect (%) ^a
	1 2 3 4 5 6 7 8 9 10 11 12 13 14 15		
MCT-2(1-15)	formyl- M T P M R K I N P L M K L I N	20.0 ± 3.39	100
MCT-2(1-14)	formyl- M T P M R K I N P L M K L I	96.7 ± 17.6	102
MCT-2(1-13)	formyl- M T P M R K I N P L M K L	186 ± 33.6	100 ± 3
MCT-2(1-12)	formyl- M T P M R K I N P L M K	633 ± 153	98 ± 3
MCT-2(1-11)	formyl- M T P M R K I N P L M	547 ± 93.9	103 ± 3
MCT-2(1-10)	formyl- M T P M R K I N P L	1,800 ± 173	98 ± 3
MCT-2(1-9)	formyl- M T P M R K I N P	10,760 ± 850	104 ± 3
MCT-2(1-8)	formyl- M T P M R K I N	41,333 ± 2,517	100 ± 2
MCT-2(1-7)	formyl- M T P M R K I	35,500 ± 500	101 ± 2
MCT-2(1-6)	formyl- M T P M R K	202,667 ± 2,309	90 ± 2**
MCT-2(1-5)	formyl- M T P M R	26,000 ± 1,581	104 ± 2
MCT-2(1-4)	formyl- M T P M	18,000 ± 1,323	88 ± 2***
Des- <i>N</i> -formyl MCT-2	M T P M R K I N P L M K L I N	>1,000,000	0
[Ala ¹]MCT-2	formyl- A T P M R K I N P L M K L I N	>10,000	70 ± 2***
[Ala ²]MCT-2	formyl- M A P M R K I N P L M K L I N	0.61 ± 0.07	106 ± 2
[Ala ³]MCT-2	formyl- M T A M R K I N P L M K L I N	16.3 ± 0.29	102 ± 1
[Ala ⁴]MCT-2	formyl- M T P A R K I N P L M K L I N	68.0 ± 2.65	100 ± 2
[Ala ⁵]MCT-2	formyl- M T P M A K I N P L M K L I N	61.3 ± 0.58	104 ± 1
[Ala ⁶]MCT-2	formyl- M T P M R A I N P L M K L I N	64.0 ± 3.00	103 ± 2
[Ala ⁷]MCT-2	formyl- M T P M R K A N P L M K L I N	94.7 ± 3.21	104 ± 2
[Ala ⁸]MCT-2	formyl- M T P M R K I A P L M K L I N	31.0 ± 3.97	106 ± 1
[Ala ⁹]MCT-2	formyl- M T P M R K I N A L M K L I N	3.02 ± 1.21	105 ± 1
[Ala ¹⁰]MCT-2	formyl- M T P M R K I N P A M K L I N	73.0 ± 13.3	100 ± 2
[Ala ¹¹]MCT-2	formyl- M T P M R K I N P L A K L I N	36.7 ± 11.0	102 ± 1
[Ala ¹²]MCT-2	formyl- M T P M R K I N P L M A L I N	12.3 ± 0.29	106 ± 3
[Ala ¹³]MCT-2	formyl- M T P M R K I N P L M K A I N	83.7 ± 3.54	107 ± 3
[Ala ¹⁴]MCT-2	formyl- M T P M R K I N P L M K L A N	76.7 ± 11.9	103 ± 3
[Ala ¹⁵]MCT-2	formyl- M T P M R K I N P L M K L I A	29.3 ± 1.49	104 ± 3

^aThe ability of each peptide to cause β-hexosaminidase release is expressed as a percentage of enzyme secretion promoted by 10 μM MCT-2(1–15). Data are expressed as the mean ± SE of four to six independent experiments. ** p < 0.01; *** p < 0.001, values significantly different from MCT-2(1–15).

from the C-terminus of MCT-2(1–15) caused consecutive increases in the EC₅₀ values without affecting the maximum response. Specifically, the EC₅₀ value of MCT-2(1–14) was increased by approximately fivefold compared with that of MCT-2(1–15) (Figure II-4B and Table II-2). MCT-2(1–13) and MCT-2(1–12) also exhibited decreased activity when compared with MCT-2(1–15), but MCT-2(1–11) had almost the same potency as MCT-2(1–12) (Figure II-4B and Table II-2). In addition, the activities of MCT-2(1–10), MCT-2(1–9), and MCT-2(1–8) were sequentially attenuated compared with that of MCT-2(1–11), but with the same maximum effect as MCT-2(1–15), and MCT-2(1–7) had almost the same potency as MCT-2(1–8). However, MCT-2(1–6), a derivative that was truncated by nine C-terminal amino acid residues, exhibited a significant decrease of the maximum response compared with MCT-2(1–15) (maximum response: 90 ± 3%) with a 5.7-fold increase in the EC₅₀ value compared with MCT-2(1–7). These results indicate that MCT-2(1–7) with an N-formyl group is the minimum structure that is required for maximum stimulation via the activation of FPR2 because the minimum sequence that gave the same level of maximum response as MCT-2(1–15) was MCT-2(1–7), which was also the minimum structure for inducing specific FPR2 activation to cause an increase of [Ca²⁺]_i (Figure II-3). In addition, the MCT-2(8–15) structure within MCT-2(1–15) may contribute to the binding affinity between MCT-2(1–15) and FPR2, since the removal of one to eight amino acid residues from the C-terminus did not affect the maximum response, but caused a consecutive increase in EC₅₀ values (Figure II-4B and Table II-2).

The effect of C-terminal truncation was examined further because MCT-2(1–6) could still induce β -hexosaminidase release. As a result, MCT-2(1–5), surprisingly, had 6.5-fold higher activity than MCT-2(1–6) (Figure II-4C and Table II-2) with the same level of maximum response as MCT-2(1–15). Moreover, the activity of MCT-2(1–4) was further reinforced compared with MCT-2(1–5) as well as MCT-2(1–6) (Table II-2); nevertheless, the maximum response of MCT-2(1–4) was significantly reduced by approximately 10% compared with MCT-2(1–15). Taken together with the observations that MCT-2(1–5) induced the activation of FPR2 and FPR1, and MCT-2(1–4) specifically activated FPR1 for the increases in $[Ca^{2+}]_i$ described above (Figure II-3), these findings suggest that MCT-2(1–5) effectively promotes the stimulation of β -hexosaminidase release via FPR1 and FPR2 activation. Furthermore, MCT-2(1–4) specifically activates FPR1 to promote stimulation.

II-4-3. Involvement of FPR1 and FPR2 in β -hexosaminidase release stimulated by MCT-2(1–15) and its derivatives

To further elucidate the involvement of FPR1 and FPR2 in β -hexosaminidase release from differentiated HL-60 cells stimulated with MCT-2(1–15) and its derivatives, I examined the inhibitory effects of inhibitors against FPR1 [cyclosporin H (CysH)] and FPR2 (PBP10) on this process. Stimulation with MCT-2(1–15) at 40 nM, which induced approximately 60% of the maximum response, was dose-dependently inhibited by PBP10, and 1 μ M PBP10 completely inhibited this activity, but 1 μ M CysH did not

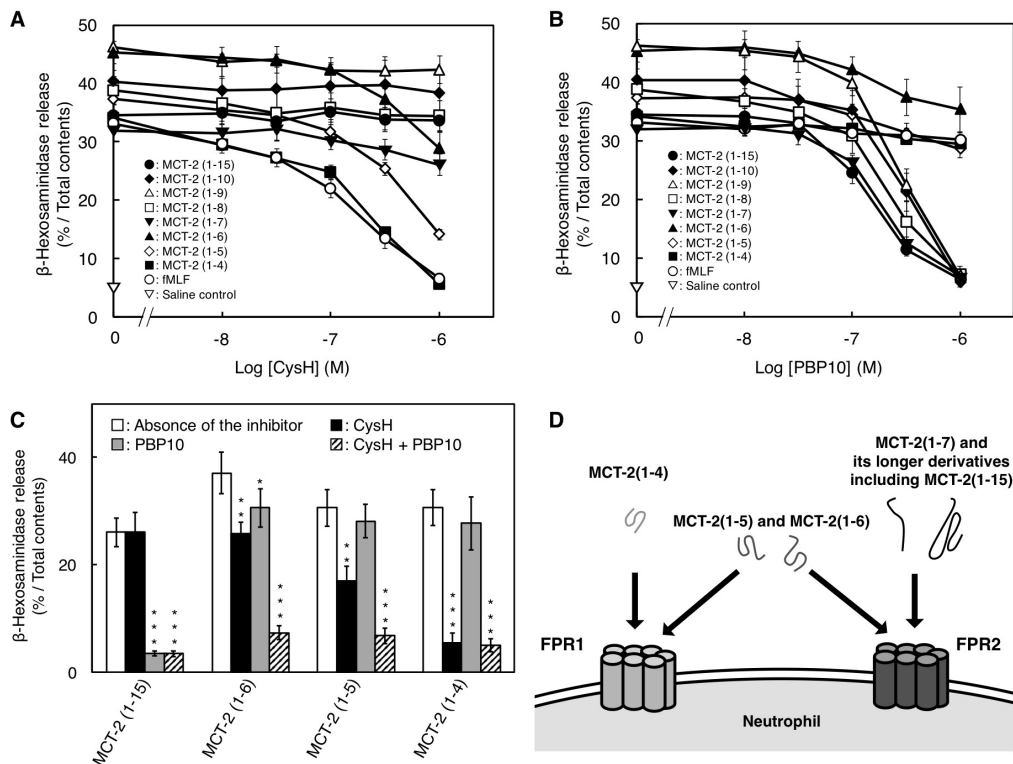


Figure II-5. Involvement of FPR1 and FPR2 in β -hexosaminidase release by differentiated HL-60 cells stimulated with MCT-2(1–15) and its derivatives. (A,B) Concentration-dependent inhibitory effects of inhibitors against FPR1 (CysH) (A) or FPR2 (PBP10) (B) on β -hexosaminidase release induced by MCT-2(1–15) and its derivatives. (C) Inhibitory effects of CysH (1 μ M; black), PBP10 (1 μ M; gray), or a combination of both inhibitors (1 μ M PBP10 and 1 μ M CysH; slash lines) on the stimulation of β -hexosaminidase release by MCT-2(1–15) and its derivatives. White bars indicate the stimulation of MCT-2(1–15) and its derivatives in the absence of the inhibitor. The stimulatory concentrations of MCT-2(1–15) and its derivatives were the concentrations that caused a 60% response of the maximum effect. The ability of each peptide in the absence or the presence of the inhibitors was expressed as a percentage of the total enzyme activity, which was the enzyme activity leaked after disruption of the cells with 0.05% Triton X-100 (%/Total). Data are expressed as the mean \pm SE of four to six independent experiments. * $p < 0.05$; ** $p < 0.01$; *** $p < 0.001$, values significantly different from each peptide in the absence of the inhibitors. (D) Receptor preference of MCT-2(1–15) and its derivatives. *N*-terminal derivatives of MCT-2 with seven amino acid residues [MCT-2(1–7)] or longer than it specifically activate FPR2, whereas MCT-2(1–4) induces the specific activation of FPR1, as well as MCT-2(1–6) and MCT-2(1–5), which activate both FPR1 and FPR2.

influence MCT-2(1–15)-induced enzyme release (Figure II-5A,B). Similarly, the responses induced by MCT-2(1–10), MCT-2(1–9), MCT-2(1–8), and MCT-2(1–7) at a concentration that caused a 60% response of the maximum effect were also abolished in a dose-dependent manner by PBP10 but not CysH (Figure II-5A,B). In contrast, stimulation with MCT-2(1–6) and MCT-2(1–5) was almost completely prevented by the combination of inhibitors (1 μ M CysH and 1 μ M PBP10) (Figure II-5C). Moreover, β -hexosaminidase release induced by MCT-2(1–4) was completely abolished by 1 μ M CysH, but was unaffected by 1 μ M PBP10 (Figure II-5A,B). These results also support the notion that MCT-2(1–7) and its longer *N*-terminal derivatives induce β -hexosaminidase release from differentiated HL-60 cells via the specific activation of FPR2; in contrast, MCT-2(1–4) specifically activates FPR1, and MCT-2(1–6) and MCT-2(1–5) activate both FPR1 and FPR2 (Figure II-5D).

II-4-4. Effects of substituting Ala for each amino acid residue of MCT-2(1–15) on β -hexosaminidase release by differentiated HL-60 cells

I examined the effect of substituting Ala for each amino acid residue in MCT-2(1–15) on the stimulation of β -hexosaminidase release to elucidate the contribution of each side chain structure to this process. As the MCT-2(1–7) structure with an *N*-formyl group was indicated as crucial for the activation of FPR2 (Figures II-3–5), I investigated the effect of substituting Ala for each amino acid residue in positions one to seven within MCT-2(1–15). The replacement of Met¹ of MCT-2(1–15) with Ala caused a 30%

reduction of the maximum response with a dramatic (>500-fold) increase in the EC₅₀ value compared with MCT-2(1–15) (Figure II-6A and Table II-2), indicating that the Met¹ side chain is important for not only the affinity of MCT-2(1–15) to FPR2, but also for FPR2 activation. The substitution of Met⁴, Arg⁵, Lys⁶, or Ile⁷ with Ala also caused an increase in the EC₅₀ value with the same level of maximum response as MCT-2(1–15). In contrast, the replacement of Thr² with Ala promoted a remarkable decrease in the EC₅₀ value without affecting the maximum response, although the substitution of Pro³ with Ala had no effect on the EC₅₀ value. These results suggest that the side chains of Met⁴, Arg⁵, Lys⁶, and Ile⁷, and Thr² within MCT-2(1–15) contribute positively and negatively, respectively, to its affinity to bind to FPR2.

I also examined the effect of substituting Ala for each amino acid residue in the MCT-2(8–15) sequence within MCT-2(1–15) because this structure may be important for the binding affinity between MCT-2(1–15) and FPR2, but not the receptor activation described above. The substitution of Leu¹⁰, Leu¹³, or Ile¹⁴ with Ala caused an increase in the EC₅₀ value with the same level of maximum response as MCT-2(1–15) (Figure II-6B and Table II-2). In contrast, the replacement of Pro⁹ with Ala promoted a remarkable decrease in the EC₅₀ value without affecting the maximum response [EC₅₀: 3 ± 2 nM, Figure II-6B and Table II-2], although the substitution of Asn⁸, Met¹¹, Lys¹², or Asn¹⁵ with Ala had no effect. These results suggest that the Leu¹⁰, Leu¹³, or Ile¹⁴, and Pro⁹ side chains within MCT-2(1–15) contribute positively and negatively, respectively,

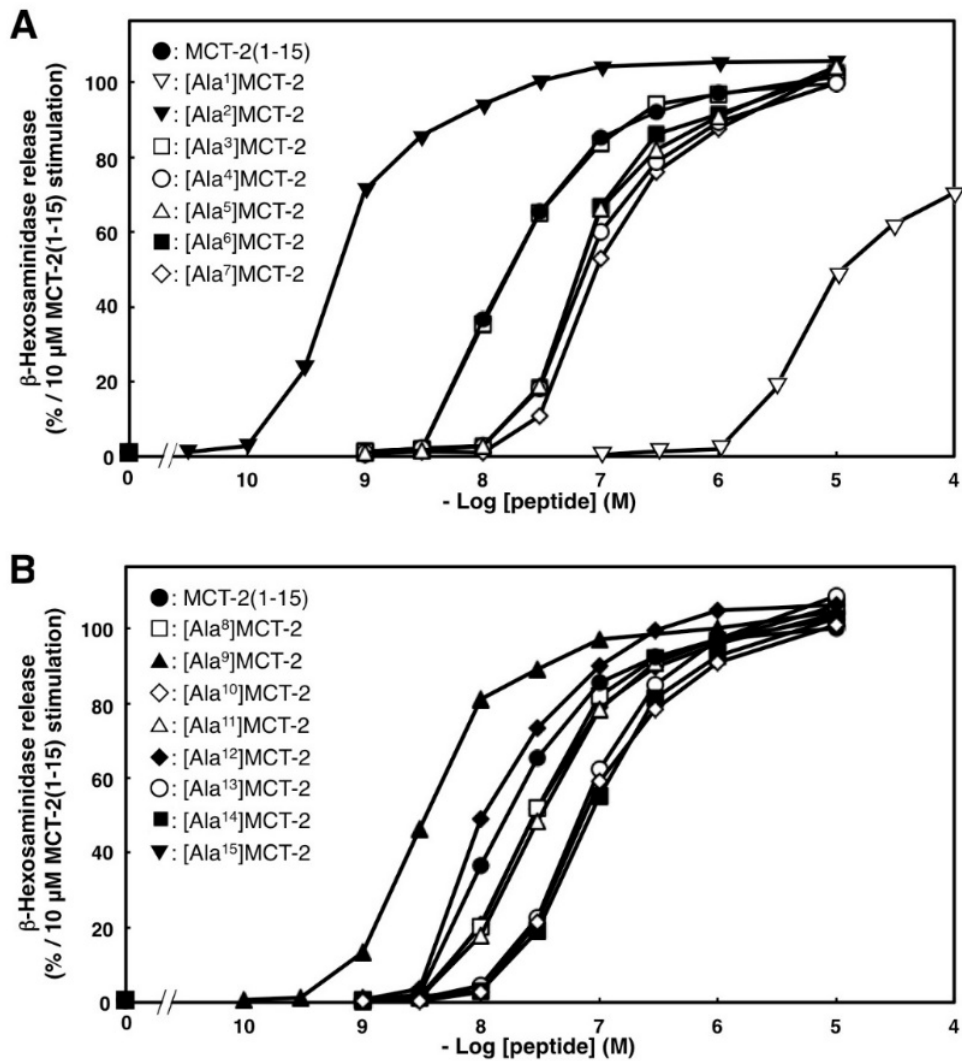


Figure II-6. Effects of substituting Ala for each amino acid residue of MCT-2(1–15) on β -hexosaminidase release by differentiated HL-60 cells. The differentiated HL-60 cells were stimulated by MCT-2(1–15) or its derivatives at 37 °C for 10 min, and the amount of the released β -hexosaminidase was quantified as described in “Materials and Methods”. The ability of each peptide to cause β -hexosaminidase release is expressed as a percentage of enzyme secretion promoted by 10 μ M MCT-2(1–15). Data are expressed as the mean \pm SE of four to six independent experiments.

to its affinity to bind to FPR2.

II-4-5. Circular dichroic spectra of MCT-2(1–15) and its derivatives

It was suggested that the Thr², Met⁴, Arg⁵, Lys⁶, Ile⁷, Pro⁹, Leu¹⁰, Leu¹³, and Ile¹⁴ side chains within MCT-2(1–15) had an effect on its binding affinity to FPR2 and that the MCT-2(8–15) structure was important for binding to FPR2. Thus, the secondary structures of MCT-2(1–15) and its derivatives were analyzed using CD spectra, which is an excellent tool for the rapid investigation of secondary structures. As described previously [48], the CD spectrum of MCT-2(1–15) exhibited two minima at 225 nm and 205 nm in TFE solution, suggesting that MCT-2(1–15) predominantly contained an α -helical structure in hydrophilic circumstance (Figure II-7A). Similarly, the spectra of the *N*-terminal MCT-2 derivatives that were truncated by one to six amino acid residues from the *C*-terminus of MCT-2(1–15) at 100 μ M also showed two minima at 225 nm and 202–208 nm in TFE solution, although these minima were consecutively attenuated by the *C*-terminal truncations (Figure II-7B–G). Moreover, the spectra of MCT-2(1–8) and MCT-2(1–7) displayed a minimum at approximately 200 nm in TFE solution (Figure II-7H,I), proposing that MCT-2(1–8) and MCT-2(1–7) do not contain defined secondary structures, even under hydrophilic conditions. In contrast, the CD spectra of all of these derivatives including MCT-2(1–15) at 100 μ M exhibited a minimum at approximately 200 nm in a hydrophilic phosphate buffer (Figure II-7), proposing that

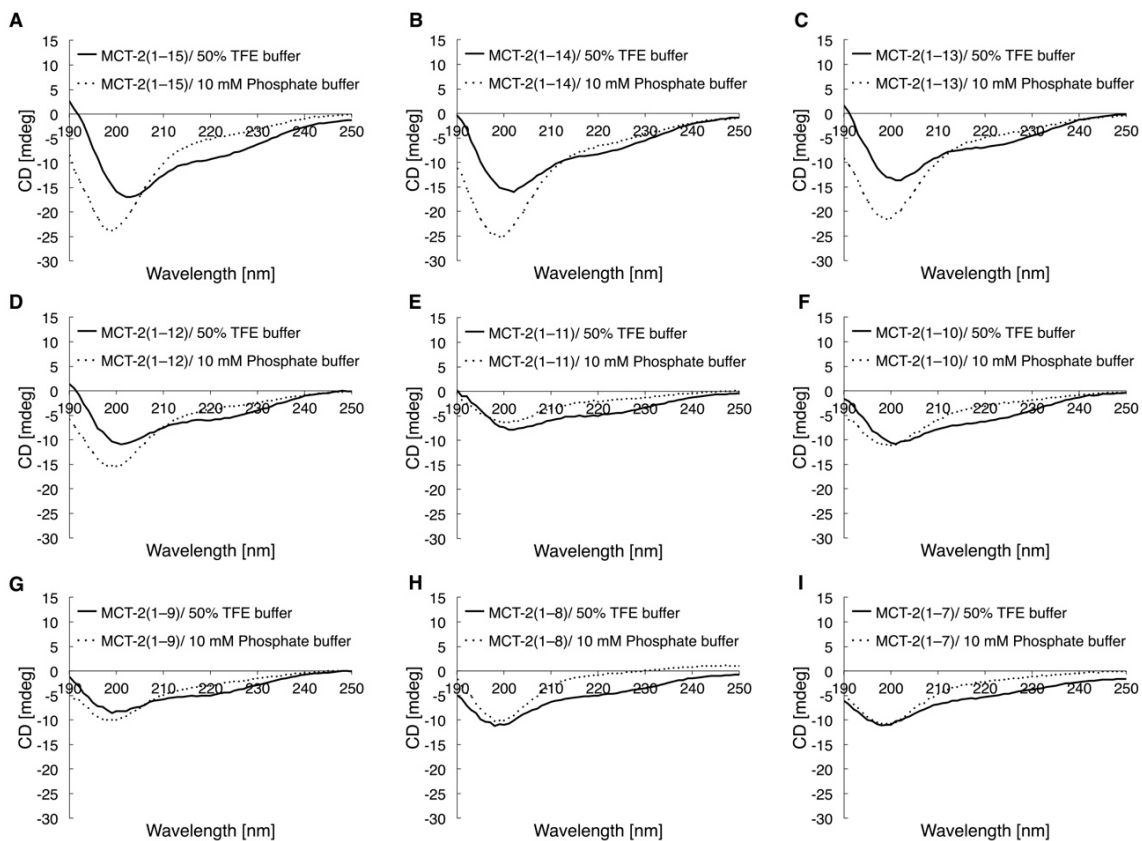


Figure II-7. CD spectra of MCT-2(1–15) and its derivatives. The CD spectra of MCT-2(1–15) (A), MCT-2(1–14) (B), MCT-2(1–13) (C), MCT-2(1–12) (D), MCT-2(1–11) (E), MCT-2(1–10) (F), MCT-2(1–9) (G), MCT-2(1–8) (H), and MCT-2(1–7) (I) in 50% TFE buffer (solid lines) or 10 mM phosphate buffer (pH 7.4) (dashed lines) were measured with a CD spectrometer. CD data with peptide solutions (final concentration: 100 μ M) were the average of five scans collected at 1 nm intervals. The results are expressed as optical rotation (mdeg).

MCT-2(1–15) and its derivatives did not form defined secondary structures in hydrophilic conditions.

II-4-6. Time-dependent alterations of the molecular forms of MCT-2(1–15) in serum

I examined the alterations of the molecular forms of MCT-2(1–15) in serum to elucidate the time-dependent degradation of MCT-2(1–15). MCT-2(1–15) was incubated with mouse serum, and the production of MCT-2-derived peptides was analyzed by RP-HPLC. The molecular masses of the newly produced peaks were measured by MALDI-TOF-MS to identify the molecular forms of the MCT-2-related peptides. As a result, the amount of MCT-2(1–15) in serum was reduced by approximately 50% and 80% at 1 and 2 h after incubation, respectively, and MCT-2(1–15) completely disappeared at 4 h (Figure II-8), indicating that its half-life in serum was approximately 1 h. In contrast, MCT-2(1–11), MCT-2(1–10), and MCT-2(1–4) were produced simultaneously with the decrease in the amount of MCT-2(1–15), that is, the production of MCT-2(1–11) and MCT-2(1–10) was detected at 1 h, and the maximum amounts of MCT-2(1–11) and MCT-2(1–10) were observed at 1 and 2 h after incubation, respectively (Figure II-8B,C). MCT-2(1–11) and MCT-2(1–10) were not found at 4 h after incubation (Figure II-8D). MCT-2(1–4) was detected initially at 1 h after incubation but at a low level, and its maximum level was observed at 4 h (Figure II-8B–F). The amount of MCT-2(1–4) was then reduced gradually over time, but it was still

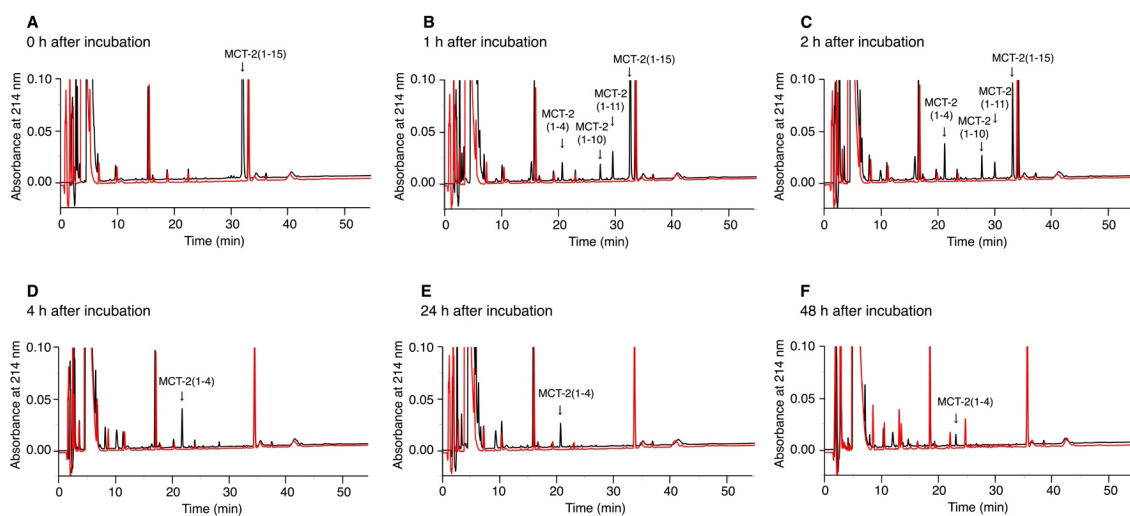


Figure II-8. Time-dependent alteration of the molecular forms of MCT-2(1–15) in serum. The alteration of the molecular forms of MCT-2(1–15) in serum was examined as described in the Materials and Methods. Briefly, MCT-2(1–15) was incubated in mouse serum at 37 °C for 0, 1, 2, 4, 24, and 48 h, and samples at those time points were analyzed by RP-HPLC. The panels show the analytical RP-HPLC profile of each sample at 0 (A), 1 (B), 2 (C), 4 (D), 24 (E), or 48 (F) h after incubation. Black and red lines indicate the samples that were incubated with and without MCT-2(1–15), respectively. Analytical conditions: column, 5C₁₈ column (4.6 × 150 mm); elution with a linear gradient from 10% to 60% CH₃CN/0.1% trifluoroacetic acid for 50 min; flow rate, 1 mL/min; detection wavelength, 214 nm. The arrows indicate the peaks containing MCT-2(1–15) or its related peptides that were identified by MALDI-TOF-MS.

present at 48 h (Figure II-8F). In addition, no fragmented peptides derived from MCT-2(1–15) were observed at any time point. These results suggest that MCT-2(1–15) is degraded by various proteases in serum, and MCT-2(1–11), MCT-2(1–10), and MCT-2(1–4) are produced simultaneously. Moreover, it is considered that MCT-2(1–4) may be produced by the degradation of MCT-2(1–15), MCT-2(1–11), or MCT-2(1–10), and was present in serum for more than 48 h. These findings suggest that MCT-2(1–15) exerts its functions not only as MCT-2(1–15) but also as MCT-2(1–11), MCT-2(1–10), and MCT-2(1–4).

II-5. Discussion

II-5-1. Recognition mechanisms of MCT-2(1–15) and its derivatives by formyl-peptide receptors

FPR1, which recognizes *N*-formylated peptides, and its homolog FPR2 are expressed in neutrophils and neutrophilic differentiated HL-60 cells [34-36, 39, 46, 50-52], and the endogenous pentadecapeptide MCT-2(1–15) specifically activates FPR2 but not FPR1 (37, 49; see also Figures II-3–6). At first, I examined the structure–activity relationships of MCT-2(1–15) to identify the minimum structure that is required for specific FPR2 activation. I found that the *N*-formyl group of MCT-2(1–15) was crucial for the induction of β -hexosaminidase release stimulated by the peptide, and suggested that the Met¹ side chain contributed not only to the affinity of MCT-2(1–15) to bind to FPR2 but also to receptor activation (Figures II-3–6).

I also showed that MCT-2(1–4), which is an *N*-terminal tetrapeptide of MCT-2(1–15), induced β -hexosaminidase release, but surprisingly, MCT-2(1–4) specifically activated FPR1 (Figures II-3–5). Specifically, the evidence that MCT-2(1–4) promoted an increase of $[Ca^{2+}]_i$ in HEK-293 cells expressing FPR1 but not in those expressing FPR2, as well as the evidence that its stimulation for β -hexosaminidase secretion was specifically inhibited by the FPR1 inhibitor CysH but not FPR2 inhibitor PBP10 indicates that MCT-2(1–4) induces β -hexosaminidase secretion in differentiated HL-60 cells via the specific activation of FPR1. In addition, MCT-2(1–5), a derivative that was extended by *C*-terminal 1 amino acid residue to MCT-2(1–4), also exhibited the induction of β -hexosaminidase release (Figure 2C), but in contrast with MCT-2(1–4),

MCT-2(1–5) caused an increase of $[Ca^{2+}]_i$ in both FPR1- and FPR2-expressing HEK-293 cells (Figure II-3F,G). These findings suggest that MCT-2(1–5) promotes β -hexosaminidase secretion via the activation of FPR1 and FPR2. The idea that MCT-2(1–5) activates FPR1 and FPR2 to induce β -hexosaminidase secretion was also supported by the use of selective inhibitors against FPR1 and FPR2; the stimulation of MCT-2(1–5) was partially inhibited by CysH or PBP10 and was completely prevented by a combination of both inhibitors (Figure II-5C).

In contrast with MCT-2(1–4) and MCT-2(1–5), MCT-2(1–7) induced β -hexosaminidase release via the specific activation of FPR2. Indeed, MCT-2(1–7) promoted β -hexosaminidase secretion in differentiated HL-60 cells and caused an increase of $[Ca^{2+}]_i$ in HEK-293 cells expressing FPR2 but not in those expressing FPR1 (Figures II-3E and II-4B). MCT-2(1–7) was also demonstrated to be a full agonist for FPR2 because the maximum response of MCT-2(1–7) to potentiate β -hexosaminidase secretion was at the same level as that induced by MCT-2(1–15), an endogenous specific agonist for FPR2. Moreover, *N*-terminal derivatives longer than MCT-2(1–7) also exhibited the same maximum effect as MCT-2(1–15) on the stimulation of β -hexosaminidase release, and those EC_{50} values were simultaneously reduced by *C*-terminal extension, that is, the activity of the derivatives was consecutively potentiated (Figure II-4B). In addition, similar to MCT-2(1–7), the *N*-terminal derivatives MCT-2(1–8), MCT-2(1–9), and MCT-2(1–10) as well as MCT-2(1–15) caused an increase of $[Ca^{2+}]_i$ only in HEK-293 cells expressing FPR2 (Figure II-3A–E). These findings indicate that the *N*-terminal derivatives longer than MCT-2(1–7) are also

specific full agonists for FPR2 to promote β -hexosaminidase secretion. This notion concerning the receptor preference of MCT-2(1–15) and its derivatives was also supported by experiments using selective inhibitors against FPR1 and FPR2. Specifically, the stimulation of β -hexosaminidase release by MCT-2(1–7) and its longer *N*-terminal derivatives was completely inhibited by the FPR2 inhibitor PBP10, but was unaffected by the FPR1 inhibitor CysH (Figure II-5A,B).

MCT-2(1–6) did not induce an increase of $[Ca^{2+}]_i$ in HEK-293 cells expressing either FPR2 or FPR1, even at 100 μ M; nevertheless, it caused β -hexosaminidase secretion (Figure II-4). The apparent discrepancy between the induction of β -hexosaminidase release and increase in $[Ca^{2+}]_i$ stimulated by MCT-2(1–6) may be a result of its weak stimulatory activity for not only FPR1, but also FPR2; the weak stimulation of β -hexosaminidase release by MCT-2(1–6) was presumably a consequence of the slight activation of both FPR1 and FPR2, although this was not evident in HEK-293 cells expressing FPR1 or FPR2. The idea that MCT-2(1–6) weakly activates FPR1 and FPR2 for the induction of β -hexosaminidase secretion was also supported by the use of selective inhibitors against FPR1 or FPR2, *i.e.*, β -hexosaminidase release stimulated by MCT-2(1–6) was partially inhibited by either CysH or PBP10, and was completely prevented by a combination of both inhibitors (Figure II-5A–C).

II-5-2. Secondary structures of MCT-2(1–15) and its derivatives for the interaction with FPR2

In the present study, I showed that the MCT-2(1–7) structure within MCT-2(1–15) is required to induce the maximum response by FPR2 activation. What is the role of the C-terminal MCT-2(8–15) sequence within MCT-2(1–15)? Truncation of one to eight amino acid residues from the C-terminus of MCT-2(1–15) had no effect on the maximum response for the stimulation of β -hexosaminidase release, but did cause a consecutive increase of EC₅₀ values (Figure II-4B and Table II-2), suggesting that the MCT-2(8–15) structure contributes to the binding affinity of MCT-2(1–15) to FPR2, but is not essential for the receptor activation itself. Especially, the removal of the Ile¹⁴, Leu¹³, Met¹¹, and Leu¹⁰ side chains from MCT-2(1–15) significantly increased the EC₅₀ values, suggesting that these hydrophobic amino acid residues are important for the affinity of MCT-2(1–15) with FPR2. Many bioactive peptides form amphipathic α -helical structures when interacting with the cell membrane, and the hydrophobic side chains of those peptides influence their affinity for the cell membrane and their receptors [53, 54]. Indeed, MCT-2(1–15) exhibited α -helical signals in CD spectra in hydrophilic conditions, and the truncation of one to eight amino acid residues from its C-terminus caused a simultaneous decrease of the α -helical signals (Figure II-7). These findings propose that the α -helical structure of MCT-2(1–15) formed in hydrophilic circumstance may also contribute to its interaction with FPR2. Here, the substitution of Pro⁹ in MCT-2(1–15) with Ala remarkably decreased the EC₅₀ value for β -hexosaminidase release, *i.e.*, its activity was potentiated by the exchange (Figure

II-6B). Taken together with our previous findings that the replacement of Pro⁹ in MCT-2(1–15) with Ala increased the α -helical content in hydrophilic conditions [48], the importance of the amphiphilic α -helical structure of the C-terminal part of MCT-2(1–15) for the improvement of its affinity for FPR2 was also supported by these results.

In this study, the Thr² side chain was also suggested to contribute negatively to the affinity of MCT-2(1–15) for FPR2, that is, the replacement of Thr² in MCT-2(1–15) with Ala promoted a remarkable decrease in the EC₅₀ value (Table 2); nevertheless, this substitution did not influence the α -helical content of MCT-2(1–15) [48]. Hence, the increase in activity by its replacement may be a result of an increase in hydrophobicity at position two that improves its binding affinity with FPR2.

II-5-3. Binding characteristics of MCT-2(1–15) and its derivatives to FPR1 and FPR2

Recently, the tertiary structure of the FPR2-G_i complex analyzed by cryo-electron microscopy (EM) has been reported, and that of the FPR1-G_i complex was also predicted based on the structure of FPR2 by Zhuang *et al.* [55]. In addition, formylated peptides containing fMLF were docked to those receptors. These findings suggested that the N-formyl groups of those peptides interacted with the Asp¹⁰⁶, Arg²⁰¹, and Arg²⁰⁵ residues distributed at the bottom of the ligand-binding cavities of FPR1 and FPR2 for the activation of both receptors. Thus, I simulated the docking of MCT-2(1–15) and its derivatives to FPR2 and FPR1 using the Glide program in Schrödinger, which was the

program used by Zhuang *et al.* [55] (Figure II-9). In brief, the *N*-formyl group of MCT-2(1–15) and its *N*-terminal derivatives longer than seven amino acid residues were also shown to interact with Asp¹⁰⁶, Arg²⁰¹, and Arg²⁰⁵ of FPR2 but not those of FPR1 because these peptides caused steric hindrance on binding to the cavity of FPR1 (Figure II-9A and C vs. Figure II-9E,G). Moreover, the Met¹ side chains of those peptides filled the space at the bottom of the ligand-binding cavity of FPR2 (Figure II-9A,C), presumably contributing to the stabilization of the interaction between the *N*-formyl groups of those peptides and Asp¹⁰⁶, Arg²⁰¹, and Arg²⁰⁵ of FPR2 for receptor activation.

In contrast, MCT-2(1–4) just fit into the binding cavity of FPR1 to promote the interaction between its *N*-formyl group and Asp¹⁰⁶, Arg²⁰¹, and Arg²⁰⁵ (Figure II-9F,H). However, the interaction between MCT-2(1–4) and the ligand-binding cavity of FPR2 was not stabilized due to the lack of hydrophobic and hydrogen bonding interactions as well as the large binding cavity (Figure II-9B,D) (docking score: FPR1–MCT-2(1–4) model, -4.84 vs. FPR2–MCT-2(1–4) model, -3.84).

In addition, the Arg⁵ or Lys⁶ residue of MCT-2(1–7) and the *C*-terminal carboxyl group of MCT-2(1–4) were exhibited to form hydrogen bonds with the Asp²⁸¹ residue of FPR2 and the Arg⁸⁴ residue of FPR1 (Figure 7C,H), respectively, which are distributed at the top of the binding cavities of those receptors, proposing that these hydrogen bonding interactions are of importance for stabilizing further receptor–peptide binding. The present simulation results can well explain those from structure–activity studies of

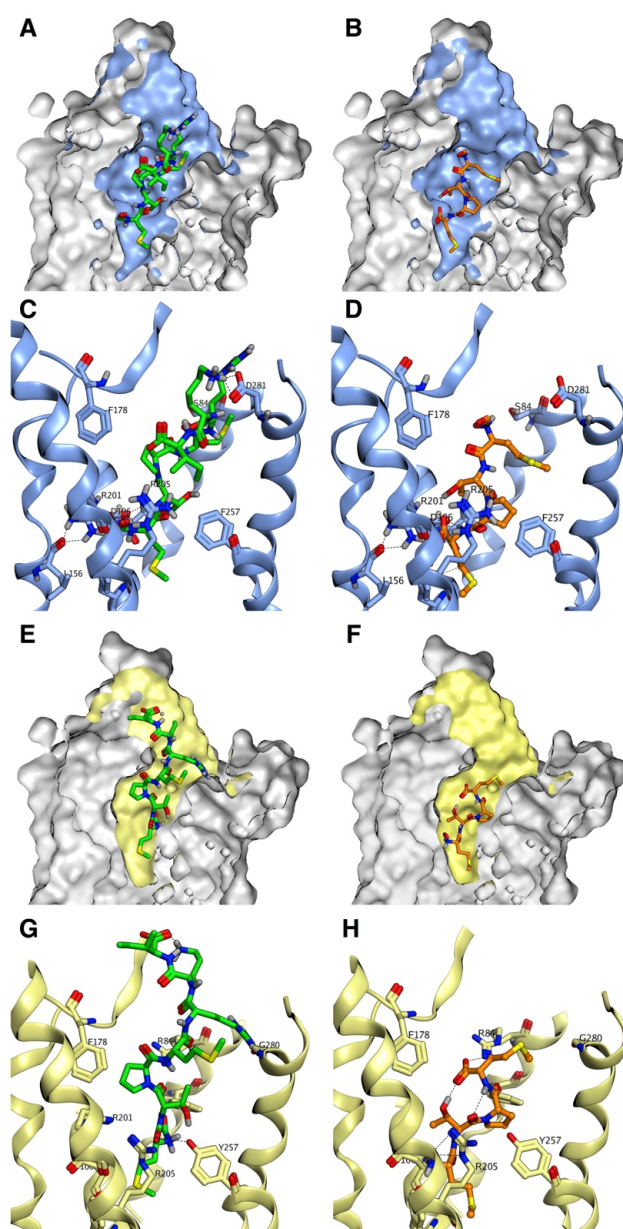


Figure II-9. Molecular docking of MCT-2(1–7) and MCT-2(1–4) to FPR2 or FPR1. MCT-2(1–7) and MCT-2(1–4) are shown as green sticks and orange sticks, respectively. (A,B) The docking model of MCT-2(1–7) (A) and MCT-2(1–4) (B) to FPR2. (C,D) Detail of the ligand-binding cavity of FPR2. The structure of the ligand-binding cavity of FPR2 is shown in blue. (E,F) The docking model of MCT-2(1–7) (E) and MCT-2(1–4) (F) to FPR1. (G,H) Detail of the ligand-binding cavity of FPR1. The structure of the ligand-binding cavity of FPR1 is shown in yellow. Hydrogen bonding interactions are shown as dashed lines.

the peptides in the present study in which MCT-2(1–7) and its derivatives longer than seven amino acid residues specifically activated FPR2, whereas MCT-2(1–4) specifically activated FPR1.

II-5-4. Alteration of the molecular forms of MCT-2(1–15) in the bloodstream

Since the receptor preference of MCT-2(1–15) and its derivatives critically depends on the length of its C-terminus, changes in the molecular forms of MCT-2(1–15) in serum were investigated. MCT-2(1–15) in serum was detected within 4 h after incubation, and its half-life was approximately 1 h (Figure II-8). In addition, the production of MCT-2-related FPR2 specific agonists MCT-2(1–11) and MCT-2(1–10) was observed at 1 h after incubation, but they were no longer present at 4 h, similar to MCT-2(1–15) (Figure II-8). Since MCT-2(1–15) is proposed to be released into the bloodstream from injury tissues as discussed below, these results suggest that MCT-2(1–15) released into the bloodstream initially activates FPR2 for several hours. In contrast, the MCT-2-related FPR1 specific agonist MCT-2(1–4) was found at low levels at 1 h after incubation; its levels then increased gradually over time, and its maximum amount was observed at 4 h. Moreover, MCT-2(1–4) was still present at 48 h (Figure II-8). These findings propose that MCT-2(1–15) released into the bloodstream is degraded and the resulting product, MCT-2(1–4), induces the activation of FPR1 following FPR2 activation and continues to activate FPR1 for over 48 h.

II-5-5. Possible physiological roles of the receptor preference shift of MCT-2(1–15) from FPR2 to FPR1

The results of this study demonstrate that the receptor preference of MCT-2(1–15) is shifted from FPR2 to FPR1 by the cleavage of its C-terminus. What is the physiological significance of this shift in receptor preference?

FPR1 and FPR2 play critical roles in inflammation including proinflammatory responses, subsequent resolution, and wound healing/tissue regeneration. Specifically, FPR1 and FPR2 are expressed mainly by inflammatory immune cells including neutrophils, monocytes, and monocyte-derived macrophage cells such as tissue-resident macrophages and microglia [36, 38, 39], and FPR2 is also expressed by a variety of cells including microvascular endothelial cells [39, 56]. FPR1 and FPR2 have roles in the mechanisms concerning the infiltration of neutrophils and macrophages into injury sites, and their activation causes various inflammatory responses, including phagocytosis, superoxide generation, and inflammatory cytokine production [36, 38, 39]. In addition, there is evidence indicating that the activation of FPR2 increases the vascular permeability of endothelial cells [39, 56], suggesting a further promotion of neutrophil infiltration from the bloodstream into injury sites following receptor activation in the initial stage of inflammation. Thus, the activation of FPR1 and FPR2 expressed by neutrophils, macrophages, and endothelial cells induces various innate immune responses initiated by the infiltration and activation of neutrophils. Oppositely, it is known that liganded FPR2 suppresses the production of inflammatory cytokines following the acute proinflammatory responses [39, 57-60]. Moreover, FPR1 activation

has been demonstrated to promote wound healing/tissue regeneration, including cell proliferation [12, 61-65].

It is believed that mitochondrial-derived *N*-formylated peptides activate FPR1 and FPR2 as endogenous activating factors. Indeed, mtDAMPs consisting of mitochondria and their contents are released into the bloodstream as a result of sterile tissue damage such as trauma [17-23], and still unidentified endogenous *N*-formylated peptides in mtDAMPs are thought to activate FPR1 and/or FPR2 to induce innate immune responses [17, 19, 30]. MCT-2(1–15) is the only endogenous *N*-formylated peptide whose chemical structure has been determined so far, and the presence of MCT-2-related peptides in mtDAMPs was recently observed by immunoblot analysis using a monoclonal antibody against MCT-2. Taken together with these findings, the present results suggest the hypothesis that MCT-2(1–15) is initially released into the bloodstream from damaged cells following tissue injury, and then activates FPR2 specifically to induce acute innate immune responses, including the infiltration and activation of neutrophils. MCT-2(1–15) is then degraded in damaged tissues as well as in the bloodstream over time, and the resulting MCT-2-related FPR1 specific agonist MCT-2(1–4) activates FPR1 to promote delayed responses, which may include resolution and wound healing/tissue regeneration (Figure II-10). Indeed, we recently found that a specific neutralizing monoclonal antibody against MCT-2 attenuated the infiltration of neutrophils into injured liver tissue in acetaminophen- or LPS-induced inflammation and prolonged the survival of mice, suggesting that MCT-2(1–15) and its

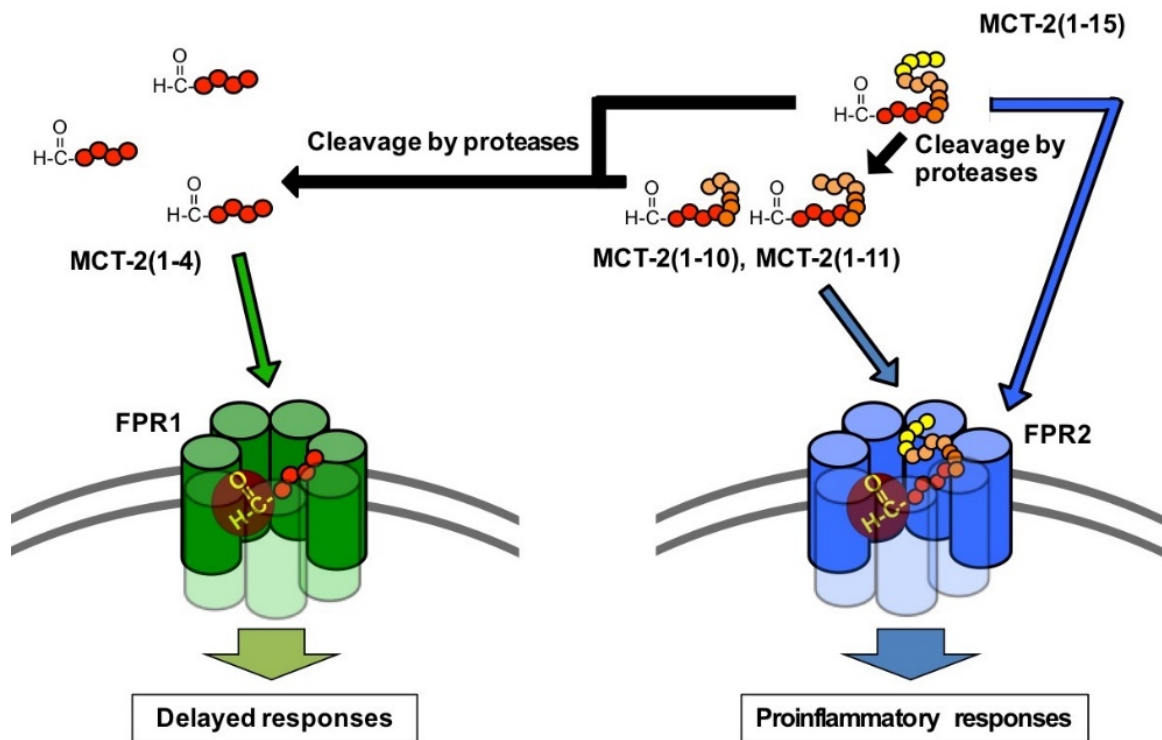


Figure II-10. Proposed mechanisms of innate immune responses involving MCT-2(1–15). MCT-2(1–15) released from damaged cells firstly activates FPR2 to induce proinflammatory responses. Released MCT-2(1–15) is then degraded over time to produce MCT-2(1–4), and the resultant MCT-2(1–4) activates FPR1 to promote delayed responses, which may be related to resolution and wound healing/tissue regeneration. See the “Discussion” in detail.

derivatives play a critical role in innate immunity. The present findings also indicate the crucial importance of investigating the molecular forms and/or exact chemical structures of those activating factors to elucidate the mechanisms underlying innate immune responses.

In conclusion, I demonstrated that FPR2 recognizes the MCT-2(1–7) structure with an *N*-formyl group for its specific activation to induce neutrophilic functions. *N*-terminal MCT-2 derivatives shorter than seven amino acid residues were shown to lose their specificity for FPR2 and gain the ability to activate FPR1. Moreover, I showed that MCT-2(1–15) was degraded in serum over time, and the MCT-2-related FPR1 specific agonist MCT-2(1–4) was produced, suggesting that the receptor preference of MCT-2(1–15) in the bloodstream is shifted from FPR2 to FPR1 over time by the cleavage of its *C*-terminus by various proteases. Thus, MCT-2 is proposed to be a factor that controls not only the initiation of innate immune responses against tissue injury, but also delayed responses via the activation of FPR1, which may relate to resolution and wound healing/tissue regeneration. In addition, because the docking simulation of MCT-2(1–15) and its derivatives to FPR1 or FPR2 well explained the receptor-specific activation mechanisms by those peptides as well as the results of structure–activity relationships, the present findings with structural information of FPR2 and FPR1 are expected to accelerate the development of specific antagonists for not only FPR2 but also FPR1 for the treatment of various inflammatory diseases including the recent epidemic of pneumonia that often causes multiple organ failure.

Chapter III
Physiological Existence of Endogenous
***N*-Formylated Peptides**

III-1. Abstract

It is known that thirteen proteins encoded in mitochondrial DNA are translated in mitochondria as *N*-formylated forms, proposing the existence of endogenous *N*-formylated peptides other than mitocryptide-2 (MCT-2). Here I investigated the effects of *N*-formylated peptides presumably cleaved from mitochondrial DNA-encoded proteins other than cytochrome *b* on the functions of neutrophilic cells in order to elucidate physiological regulations by endogenous *N*-formylated peptides in innate immunity. Four *N*-formylated peptides derived from cytochrome *c* oxidase subunit I and NADH dehydrogenase subunits 4, 5, and 6 among twelve peptides derived from mitochondrial DNA-encoded proteins efficiently induced not only migration but also β -hexosaminidase release, which is an indicator of phagocytosis in HL-60 cells differentiated into neutrophilic cells with the activities that were comparable to or higher than those induced by MCT-2. These findings suggest that not only MCT-2 but also those *N*-formylated peptides presumably cleaved from mtDNA-encoded proteins regulate innate immune responses.

III-2. Introduction

Recently, mitochondrial damage-associated molecular patterns (mtDAMPs) are paid much attention as pro-inflammatory factors in sterile inflammation that were caused by internal tissue damages including ischemic injuries/infarction, trauma, and burn [17-23]. mtDAMPs are demonstrated to be released from those tissue injury sites, and are shown to induce neutrophil migration and activation. One family of activating factors contained in mtDAMPs is believed to be endogenous *N*-formylated peptides, although they have not been molecularly specified yet. It is considered that MCT-2 is a first-line candidate as a peptidergic activating factor in mtDAMPs, since it is an only endogenous neutrophil-activating *N*-formylated peptide that has been isolated and identified from mammalian tissues so far [14]. Moreover, endogenous *N*-formylated peptides other than MCT-2 possibly exist as activating factors in mtDAMPs since thirteen proteins including cytochrome *b* encoded in mitochondrial DNA are known to be translated in mitochondria as *N*-formylated forms [40, 41].

In this chapter, I predicted endogenous *N*-formylated peptides that are produced from mtDNA-encoded proteins and investigated their effects on the functions of neutrophilic cells in order to elucidate the possible existence of endogenous *N*-formylated peptides other than MCT-2 for the induction of innate immune responses.

III-3. Materials and Methods

III-3-1. Prediction and synthesis of endogenous N-formylated peptides

The sequences of thirteen proteins that are encoded in human mtDNA were obtained from protein data base SWISS-PROT, and endogenous *N*-formylated peptides other than MCT-2 were basically predicted from those sequences in accordance with the information regarding cleavage sites of trypsin or chymotrypsin within *N*-terminal soluble domains of the mtDNA-encoded proteins. The peptides were synthesized by a solid-phase method using a 9-fluorenylmethyloxycarbonyl strategy as described in Chapter II.

III-3-2. β -Hexosaminidase release and chemotaxis assay

HL-60 cells (RIKEN Cell Bank, Ibaraki, Japan) were cultured and differentiated into neutrophilic/granulocytic cells as described in Chapter II. The ability of peptides on the stimulation of β -hexosaminidase release from HL-60 cells differentiated into neutrophilic/granulocytic cells was assessed following the method described in Chapter II-3-5.

The chemotactic activity of peptides was measured using ChemotaxiCell chambers (pore size of filter membrane: 3 μ m; Kurabo, Osaka, Japan) as described elsewhere [13, 14]. Briefly, the differentiated cells were washed three times with HEPES-buffered Hank's solution (HBHS; 10 mM HEPES, 136.9 mM NaCl, 5.4 mM KCl, 1.2 mM CaCl₂, 0.44 mM KH₂PO₄, 0.49 mM MgCl₂, 0.41 mM MgSO₄, 0.34 mM Na₂HPO₄, 5.5 mM glucose, 4.2 mM NaHCO₃, and 0.1% BSA, pH 7.4) and then

resuspended in HBHS to a density of 2×10^6 cells/ml. After preincubation at 37°C for 10 min, 500 μ L of the cell suspension was transferred to a ChemotaxiCell chamber (1×10^6 cells/chamber). The chambers were placed in each well of a 24-well microplate, in which each well contained 1 mL of preheated (37°C) HBHS containing stimulating peptides, and incubated at 37°C for 1 h. The chambers were then removed from the plate, and the cells in the lower wells were counted. The ability of each peptide to induce migration was expressed as a chemotaxis index, which is the number of cells that migrated after stimulation divided by the number of cells that migrated after vehicle treatment.

III-3-5. Statistical analysis

Data are expressed as the mean \pm standard error (SE) in experiments containing multiple data points.

III-4. Result

III-4-1. Prediction of endogenous N-formylated peptides derived from mtDNA-encoded proteins

I predicted *N*-formylated peptides presumably produced from mtDNA-encoded proteins utilizing the information of cleavage sites for trypsin and chymotrypsin within the *N*-terminal soluble domains as described in “Materials and Methods”. Five *N*-formylated peptides were predicted from cytochrome *c* oxidase subunit I (COX1), and III (COX3), and NADH dehydrogenase subunit 2 (ND2), 4 (ND4), and 5 (ND5) (Table III-1). In case of *N*-formylated peptides derived from cytochrome *c* oxidase subunit II (COX2) and ATP synthase subunit protein 6 (ATP6), it was predicted from the information of cleavage sites for chymotrypsin in the transmembrane regions next to the *N*-terminal soluble domains, since COX2 and ATP6 did not have cleavage sites for trypsin and chymotrypsin within the *N*-terminal soluble domains (Table III-1). *N*-formylated peptides derived from NADH dehydrogenase subunit 4L (ND4L) and 6 (ND6) were also foretold by the information regarding cleavage sites for chymotrypsin within the *N*-terminal transmembrane regions, because ND4L and ND6 did not have *N*-terminal soluble domains (Table III-1). As NADH dehydrogenase subunit 1 (ND1) and ATP synthase subunit protein 8 (ATP8) did not contain cleavage sites for trypsin and chymotrypsin within the *N*-terminal soluble domain or the transmembrane region next to the *N*-terminal soluble domain (Table III-1), *N*-formylated peptides derived from those proteins were designed as peptides having around ten amino acid residues.

Table III-1. *N*-terminal sequences of thirteen proteins that are encoded in human mtDNA, and their cleavage sites of trypsin or chymotrypsin.

Protein	N-terminal sequence				
	1	10	20	30	40
	Physiological cleavage				
CYB	formyl-MTPMRKINPLMKLIN	HSF	IDLPTPSN	ISAWWN	FGSLLGAC
	TRY	TRY	CHY		
COX1	formyl-MFADRWLFSTNHKDI	GTLYL	LLFGAWAGV	LGTA	LSLLIRAE
			CHY		
COX2	formyl-MAHAAQVGLQDATSP	IMEEL	ITF	HDHALMI	IFLICFLVLY
	TRY				
COX3	formyl-MTHQSHAYHMKPSP	WPL	TGALSALL	MTSGLAMW	FHFHSM
ND1	formyl-MPMANLLLLIVPIL	IA	MAFLML	TERKILGYM	QLRKGPNVV
		CHY	CHY		
ND2	formyl-MNPLAQPV	IYST	IFAGTL	ITALSSHWFF	TWVGLEMNMLAF
ND3	formyl-MNFALILMINTLL	LALLMII	TFWLPQL	NGYMEKSTPY	ECG
	CHY	CHY			
ND4L	formyl-MPLIYMN	I	LAFTISLLGML	VYRSHLMS	SLLCLEGMMLSL
	TRY		TRY	TRY	
ND4	formyl-MLKLI	VP	TIMLLPL	TWLSKK	HMIWINTTTHSLIISIPLL
				TRY	
ND5	formyl-MTMHTTMTTL	TL	TSLIPP	ILTTLVNP	NKKN
					TRY
ND6	formyl-MMYALF	LLSVGL	VMGFVGFSS	SKPSPI	YGGLVLIVSGVVGC
	CHY	CHY			
ATP6	formyl-MNENL	FASFI	A	P	TILGLPAAVLIILFP
	CHY	CHY			
ATP8	formyl-MPQLNTT	VWP	TMITP	MLLTL	FLITQLKMLNTNYHLPPSPK

The red and black arrows indicate the cleavage sites of trypsin (TRY) and chymotrypsin (CHY), respectively. The membrane domains of proteins are shown in yellow. The red characters indicate the sequences of predicted *N*-formylated peptides.

I synthesized an *N*-formylated peptide derived from NADH dehydrogenase subunit 3 (ND3) as a *N*-terminal pentapeptide, because ND3 neither has the *N*-terminal soluble domain nor cleavage sites for trypsin or chymotrypsin within the *N*-terminal transmembrane regions that ND3 has, and an *N*-terminal decapeptide from ND3 was insoluble in physiological buffers. Those predicted *N*-formylated peptides were shown in Table III-2.

III-4-2. β -Hexosaminidase release from neutrophilic/granulocytic differentiated HL-60 cells induced by predicted *N*-formylated peptides

The ability of predicted peptides as well as MCT-2 to induce β -hexosaminidase release from neutrophilic/granulocytic differentiated HL-60 cells was examined to elucidate whether those *N*-formylated peptides can induce neutrophilic functions. As described in Chapter II, MCT-2 induced β -hexosaminidase release from differentiated HL-60 cells (EC_{50} : MCT-2, 25 ± 2 nM, Figure III-1), and exhibited the maximum response at concentrations greater than 1 μ M. Similar to MCT-2, COX1(1–13), ND4(1–20), ND5(1–28), and ND6(1–6) efficiently induced β -hexosaminidase release (EC_{50} 's: COX1 (1–13), 1.8 ± 0.2 nM; ND4 (1–20), 3.3 ± 0.3 nM; ND5 (1–28), 10.2 ± 1.1 nM; ND6 (1–6), 4.3 ± 0.1 nM, Figure III-1), and their maximum responses were the same level that was induced by MCT-2. COX2(1–23), COX3(1–12), ND2(1–10), ND3(1–5), and ND4L(1–5) also caused β -hexosaminidase secretion with the same level

Table III-2. Primary structures of predicted *N*-formylated peptides derived from mtDNA-encoded proteins.

Peptide	Sequence		
	1	10	20
COX1(1-13)	formyl-MFADRWLFSTNHK		
COX2(1-23)	formyl-MAHAAQVGLQDATSPIMEELITF		
COX3(1-12)	formyl-MTHQSHAYHMK		
ND1(1-10)	formyl-MPMANLLLLLI		
ND2(1-10)	formyl-MNPLAQPVIY		
ND3(1-5)	formyl-MNFAL		
ND4L(1-5)	formyl-MPLIY		
ND4(1-20)	formyl-MLKLIVPTIMLLPLTWLSKK		
ND5(1-28)	formyl-MTMHTTMTTLTLTSLIPPILTTLVNPBK		
ND6(1-6)	formyl-MMYALF		
ATP6(1-9)	formyl-MNENLFASF		
ATP8(1-11)	formyl-MPQLNTTVWPT		

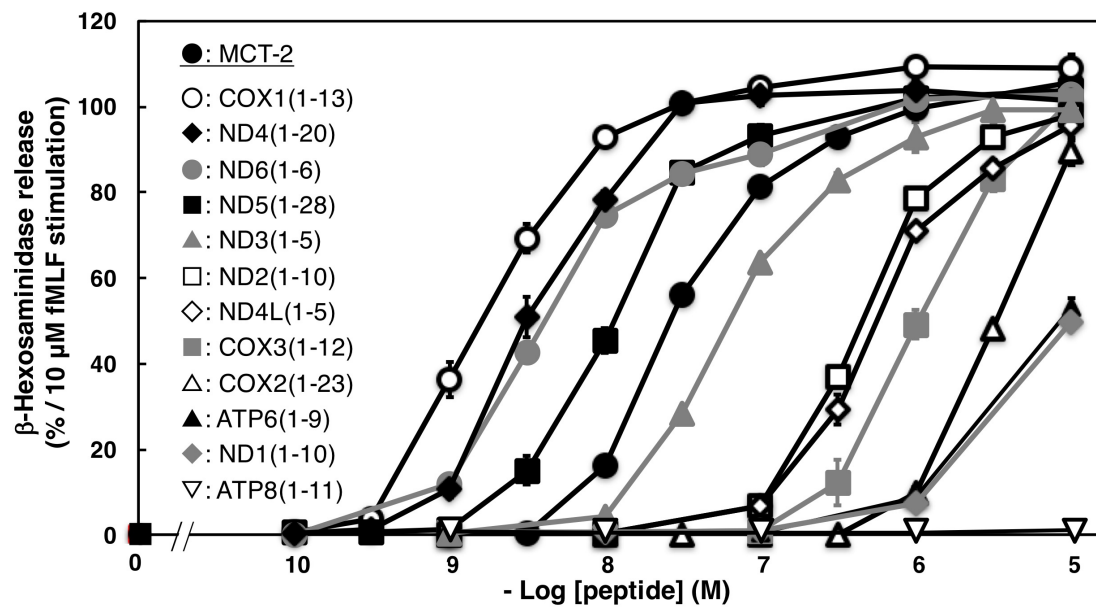


Figure III-1. β -Hexosaminidase release from differentiated HL-60 cells induced by *N*-formylated peptides predicted from mtDNA-encoded proteins. The ability of each peptide to induce β -hexosaminidase release is expressed as a percentage of enzyme secretion promoted by 10 μ M fMLF. Data are expressed as the average of four to seven independent experiments.

of the maximum responses as MCT-2, but their EC₅₀ values were significantly higher than that of MCT-2 (EC₅₀'s: COX2(1–23), 3,267 ± 123 nM; COX3(1–12), 1,025 ± 95 nM; ND2(1–10), 420 ± 9 nM; ND3(1–5), 59 ± 4 nM; ND4L(1–5), 483 ± 18 nM, Figure III-1). ND1(1–10). ATP6(1–9) also promoted β-hexosaminidase secretion (EC₅₀'s: ND1(1–10), >10,000 nM; ATP(1–9), >10,000 nM, Figure III-1), although their maximum responses were lower than that of MCT-2. ATP8(1–11) did not induce β-hexosaminidase release even at a concentration of 100 μM.

III-4-3. Migration of differentiated HL-60 cells induced by predicted N-formylated peptides

COX1(1–13), ND4(1–20), ND5(1–28), and ND6(1–6) as well as MCT-2 that effectively induce β-hexosaminidase release (Figure III-1) were further examined for their ability to promote chemotaxis in differentiated HL-60 cells. MCT-2 promoted chemotaxis of differentiated HL-60 cells with the maximum response at 10 nM, and the promotion was completely desensitized at 1 μM as described previously (14; Figure III-2). Similarly, COX1(1–13), ND4(1–20), ND5(1–28), and ND6(1–6) induced the chemotaxis in a bell shaped manner. Namely, COX1(1–13) and ND5(1–28) showed the maximum responses at 1 nM for the chemotactic stimulation, but the responses were completely suppressed at 10 nM and 100 nM, respectively (Figure III-2). ND6(1–6) also induced neutrophilic migration with the maximum response at 3 nM, and the effect

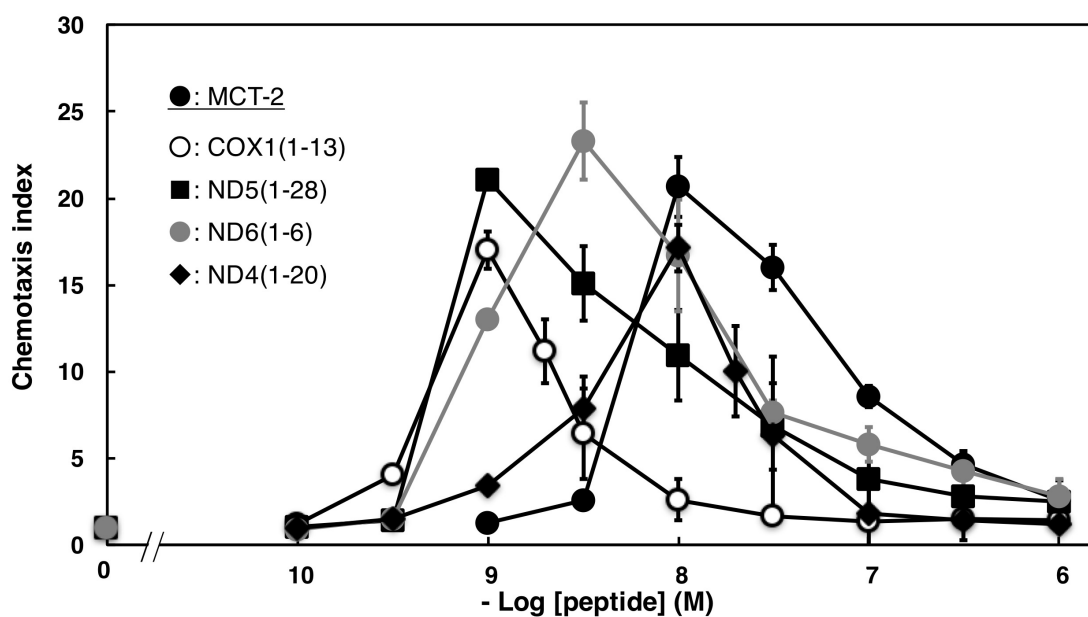


Figure III-2. Migration of differentiated HL-60 cells induced by MCT-2, COX1 (1–13), ND4 (1–20), ND5 (1–28), and ND6 (1–6). The activity is expressed as a chemotaxis index, which is the number of cells that migrated after stimulation divided by the number of cells that migrated after vehicle treatment. Data are expressed as the average of four independent experiments.

was completely diminished at 1 μ M (Figure III-2). ND4(1-20) promoted the chemotaxis with the maximum response at 10 nM, and the induction was completely desensitized at 100 nM (Figure III-2). These results demonstrate that predicted peptides COX1(1-13), ND4(1-20), ND5(1-28), and ND6(1-6) have the almost same ability to MCT-2 on chemotaxis of differentiated HL-60 cells.

III-5. Discussion

Since thirteen proteins including cytochrome *b* are encoded in mtDNA and translated in mitochondria as *N*-formylated forms [40, 41], it is possible that endogenous *N*-formylated peptides other than MCT-2 are also produced and regulate physiological and/or pathophysiological functions in innate immunity. In order to evaluate this possibility, putative endogenous *N*-formylated peptides from the mtDNA-encoded proteins were examined for their abilities to activate neutrophilic cells. Namely, endogenous *N*-formylated peptides other than MCT-2 were predicted from sequences of the twelve proteins that are encoded in human mtDNA utilizing information regarding putative cleavage sites of trypsin and chymotrypsin. Among those twelve *N*-formylated peptides, four peptides derived from COX1, ND4, ND5, and ND6, whose primary structures are shown in Table III-2, induced β -hexosaminidase release efficiently with the promotion of chemotaxis over the concentration range of 1–3 nM, 3–30 nM, 1–30 nM, and 1–300 nM, respectively (Figure III-1 and III-2). These findings suggest that not only MCT-2 but also those predicted *N*-formylated peptides presumably cleaved from COX1, ND4, ND5, and ND6 regulate innate immune responses including neutrophil infiltration and activation.

It has been shown that mtDAMPs consisting of mitochondria and their contents are released into the bloodstream from injured cells in sterile tissue damage sites such as trauma and burn [17-23], and the released mtDAMPs induce innate immune responses including neutrophil migration and activation [17, 19, 23, 30, 31]. One family of such inducing factors is thought to be endogenous *N*-formylated peptides. MCT-2 should be

one of such factors in mtDAMPs, because not only MCT-2 exhibits efficient functional abilities to neutrophils but also the presence of its related peptides in mtDAMPs has been recently found using a specific monoclonal antibody against MCT-2 [manuscript in preparation]. Moreover, it is highly possible that four *N*-formylated peptides COX1(1–13), ND4(1–20), ND5(1–28), and ND6(1–6) that show the potencies comparable to MCT-2 also involve innate immunity as activating factors in mtDAMPs.

For the receptors for such endogenous *N*-formylated peptides, FPR1 and FPR2 are known to be expressed by immune cells including neutrophils and macrophages [36, 38, 39]. FPR1 and FPR2 are also expressed by a variety of non-immune cells such as endothelial cells, epithelial cells, and hepatocytes [39, 56, 61-63, 65], and those receptors are suggested to be involved in innate immune responses. Regarding receptor preferences of such endogenous *N*-formylated peptides, MCT-2 has been shown to specifically activate FPR2 but not FPR1 as described in Chapter II. Moreover, we have also investigated the receptor molecules for COX1(1–13), ND4(1–20), ND5(1–28), and ND6(1–6) by the collaboration with Forsman's group at University of Gothenburg; ND4(1–20) and ND5(1–28) specifically activate FPR2, whereas ND6(1–6) specifically induces the activation of FPR1, and COX1(1–13) promotes the activation of both FPR1 and FPR2 [66]. However, receptors for those *N*-formylated peptides may be affected by their molecular forms because the receptor molecule for MCT-2 is shifted from FPR2 to FPR1 by the alterations of its molecular forms as shown in Chapter II. The physiological roles of endogenous *N*-formylated peptides and their regulatory mechanisms in innate immunity therefore should be investigated with the consideration

of their receptor preferences that may be changed depending on their molecular forms.

Chapter IV
General conclusions

For a long time, it had been unclear what factors induce initial migration and activation of neutrophils after sterile tissue damage such as ischemia reperfusion injury. Mitocryptides, a novel family of neutrophil-activating peptides derived from various mitochondrial proteins including MCT-1, MCT-2 and MCT-CYC have been purified and identified from mammalian tissues for candidate factors that promote such immediate neutrophilic functions [13-15]. These mitocryptides can be categorized into two groups, that is, *N*-formylated peptide MCT-2 [14] and non-formylated peptides such as MCT-1 and MCT-CYC [13, 15]. Here, I investigated the structure–activity relationships of MCT-2 to elucidate how MCT-2 are specifically recognized by its receptor molecule FPR2 expressed in neutrophilic cells. I demonstrated that the MCT-2(1–7) sequence with an *N*-formyl group was a minimum structure for the specific activation of FPR2. Moreover, it was shown that the receptor of MCT-2 was surprisingly shifted from FPR2 to its homologue FPR1 by its physiological *C*-terminal cleavages. These results propose that MCT-2 firstly activates FPR2 to induce proinflammatory responses and later promotes delayed responses presumably including wound healing/tissue regeneration via FPR1 activation. I also examined the physiological existence of endogenous *N*-formylated peptides other than MCT-2, and four *N*-formylated peptides COX1(1–13), ND4(1–20), ND5(1–28), and ND6(1–6) were shown to efficiently induce the migration and phagocytosis of neutrophilic cells with potencies comparable to or higher than MCT-2. These findings suggest that those four *N*-formylated peptides are also involved in the regulation of innate immune responses.

Recently, mitochondrial damage-associated molecular patterns (mtDAMPs) have

been focused on as pro-inflammatory factors in innate immunity [17-23]. Indeed, mitochondria and their contents are released from various tissues damaged by not only sterile inflammation but also bacterial infection for the promotion of innate immune responses. One family of such activating factors that induce innate immune responses is considered to be endogenous *N*-formylated peptides. Recently, we found the presence of MCT-2-like immunoreactivity in mtDAMPs using a specific monoclonal antibody against MCT-2 [manuscript in preparation]. In this thesis, I showed that not only MCT-2 but also ND6(1–6), ND5(1–28), ND4(1–20), and COX1(1–13) exhibited efficient potencies in neutrophilic migration and activation. These findings suggest that those *N*-formylated peptides including MCT-2 are peptidergic factors that induce innate immune responses in mtDAMPs.

Although it is suggested the physiological roles of *N*-formylated peptides including MCT-2 in mtDAMPs, are the peptidergic factors contained in mtDAMPs only *N*-formylated peptides? As described above, non-formylated peptides MCT-1 and MCT-CYC can also efficiently induce not only neutrophilic chemotaxis but also phagocytosis at nanomolar concentrations [13, 15]. Moreover, it was found that most fragmented peptides derived from mitochondrial transit sequences in nuclear-encoded mitochondrial proteins showed the abilities to induce neutrophil migration and activation efficiently [16]. Recently, it was also observed that the mixture of these mitocryptides at the concentrations that do not cause the stimulation by each peptide markedly induced phagocytosis in neutrophilic cells, suggesting that neutrophils are concertedly activated by accumulation of various mitocryptides [67]. This synergistic

signaling mechanism has been designated as "accumulative signaling" [67, 68]. These findings suggest the hypothesis that abundant accumulation of various mitocryptides existing in mtDAMPs concertedly causes severe and complicated inflammation-associated neutrophilic functions. Thus, it is important to investigate the involvement of *N*-formylated mitocryptides and non-formylated ones in not only sterile inflammation but also bacterial infection for the elucidation of the complete figure of the "very" early stage of innate immune responses. We are now attempting to elucidate physiological and pathophysiological roles of those mitocryptides utilizing their specific neutralizing monoclonal antibodies [68-70]. We are also investigating the signaling mechanisms promoted by various mitocryptides including dynamic cellular movements of receptors and signaling molecules [71-75]. The elucidation of not only physiological and pathophysiological roles but also signaling mechanisms concerning those mitocryptides are expected to provide therapeutic breakthrough for various inflammatory diseases such as multiple organ failure [75].

Acknowledgements

I express my deepest gratitude and sincere, wholehearted appreciation to Professor Dr. Hidehito Mukai (Laboratory of Peptide-Science, Graduate School of Bio-Science, Nagahama Institute of Bio-Science and Technology) for his kind guidance, constructive support, and hearty encouragement provided throughout this study. In addition, I feel honored to have been given the opportunity to study not only peptide science but also biochemistry and pharmacology from the beginning.

I wish to express my sincere and heartfelt gratitude to Professor Dr. Yasushi Kawai, Professor Dr. Osamu Saitoh, and Professor Dr. Shintaro Nomura (Nagahama Institute of Bio-Science and Technology) for their kind support, constructive discussions, constant encouragement, and their careful perusing of my original manuscript.

I am also indebted to Professor Dr. Yoshiaki Kiso for valuable discussion, encouragement and support during this study.

I also thank Associate Professor Dr. Masafumi Shionyu for helpful discussions and suggestions related to the docking between MCT-2 or its derivatives and FPR2 or FPR1.

I am also grateful to Dr. Tatsuya Hattori, Koki Tsutsumi, Kodai Nishino, Shinichiro Tamura, Koji Ohura, Keisuke Kamada, Tomoyuki Miyaji, Hiroki Hirai, Ryota Tanemura, Yusuke Koike, Akihiko Harada, and all other colleagues in Laboratory of Peptide Science, Graduate School of Bio-Science, Nagahama Institute of Bio-Science and Technology, for their valuable comments and for their assistance and cooperation in various experiments.

I would like to appreciate to Japan Society for the Promotion of Science for the support of this research.

Finally, my special thanks goes to my family and friends for warm support and encouragement.

References

1. Springer, T. A. (1994) Traffic signals for lymphocyte recirculation and leukocyte emigration: The multistep paradigm. *Cell* **76**, 301-314.
2. Lay, K. (1996) Molecular mechanisms of leukocyte recruitment in the inflammatory process. *Cardiovasc Res* **32**, 733-742.
3. Kolaczkowska, E., and Kubes, P. (2013) Neutrophil recruitment and function in health and inflammation. *Nat Rev Immunol* **13**, 159-175.
4. Schiffmann, E., Corcoran, B. A., and Wahl, S. M. (1975) N-formylmethionyl peptides as chemoattractants for leucocytes. *Proc Natl Acad Sci USA* **72**, 1059-1062.
5. Marasco, W. A., S. H. Phan, S. H., Krutzsch, H., Showell, H. J., Feltner, D. E., Nairn, R., Becker, E. L., and Ward, P. A. (1984) Purification and identification of formyl-methionyl-leucyl-phenylalanine as the major peptide neutrophil chemotactic factor produced by *Escherichia coli*. *J Biol Chem* **259**, 5430-5439.
6. Rot, A., Henderson, L. E., Copeland, T. D., and Leonard, E. J. (1987) A series of six ligands for the human formyl peptide receptor: tetrapeptides with high chemotactic potency and efficacy. *Proc Natl Acad Sci USA* **84**, 7967-7971.
7. Carp, H. (1982) Mitochondrial N-formylmethionyl proteins as chemoattractants for neutrophils. *J Exp Med* **155**, 264-275.
8. Becker, E. L. (1972) The relationship of the chemotactic behavior of the complement-derived factors, C3a, C5a, and C567, and a bacterial chemotactic factor to their ability to activate the proesterase 1 of rabbit polymorphonuclear leukocytes. *J Exp Med* **135**, 376-387.
9. Fernandez, H. N., Henson, P. M., Otani, A., and Hugli, T. E. (1978) Chemotactic response to human C3a and C5a anaphylatoxins. I. Evaluation of C3a and C5a leukotaxis in vitro and under stimulated in vivo conditions. *J Immunol* **120**, 109-115.
10. Walz, A., Peveri, P., Aschauer, H., and Baggiolini, M. (1987) Purification and amino acid sequencing of NAF, a novel neutrophil-activating factor produced by

monocytes. *Biochem Biophys Res Commun* **149**, 755-761.

11. Baggiolini, M., Walz, A., and Kunkel, S. L. (1989) Neutrophil-activating peptide-1/interleukin 8, a novel cytokine that activates neutrophils. *J Clin Invest* **84**, 1045-1049.
12. Liu, M., Chen, K., Yoshimura, T., Liu, Y., Gong, W., Le, Y., Gao, J. L., Zhao, J., Wang, J. M., Wang, A. (2014) Formylpeptide receptors mediate rapid neutrophil mobilization to accelerate wound healing. *PLoS One* **9**, e90613.
13. Mukai, H., Hokari, Y., Seki, T., Takao, T., Kubota, M., Matsuo, Y., Tsukagoshi, H., Kato, M., Kimura, H., Shimonishi, Y., Kiso, Y., Nishi, Y., Wakamatsu, K., and Munekata, E. (2008) Discovery of mitocryptide-1, a neutrophil-activating cryptide from healthy porcine heart. *J Biol Chem* **283**, 30596-30605.
14. Mukai, H., Seki, T., Nakano, H., Hokari, Y., Takao, T., Kawanami, M., Tsukagoshi, H., Kimura, H., Kiso, Y.; Shimonishi, Y., Nishi, Y., and Munekata, E. (2009) Mitocryptide-2: purification, identification, and characterization of a novel cryptide that activates neutrophils. *J Immunol* **182**, 5072-5080.
15. Hokari, Y., Seki, T., Nakano, H., Matsuo, Y., Fukamizu, A., Munekata, E., Kiso, Y., and Mukai, H. (2012) Isolation and identification of novel neutrophil-activating cryptides hidden in mitochondrial cytochrome c. *Prot Pept Lett* **19**, 680-687.
16. Ueki, N., Someya, K., Matsuo, Y., Wakamatsu, K., and Mukai, H. (2007) Cryptides: functional cryptic peptides hidden in protein structures. *Biopolymers (Pep Sci)* **88**, 190-198.
17. Zhang, Q., Raouf, M., Chen, Y., Sumi, Y., Sursal, T., Junger, W., Brohi, K., Itagaki, and K., Hauser, C. (2010) Circulating mitochondrial DAMPs cause inflammatory responses to injury. *Nature* **464**, 104-107.
18. McDonald, B., Pittman, K., Menezes, G. B., Hirota, S. A., Slaba, I., Waterhouse, C. C. M., Beck, P. L., Muruve, D. A., and Kubes, P. (2010) Intravascular danger signals guide neutrophils to sites of sterile inflammation. *Science* **330**, 362-366.
19. Hauser, C. J., Sursal, T., Rodriguez, E. K., Appleton, P. T., Zhang, Q., and Itagaki, K.

- (2010) Mitochondrial DAMPs from femoral reamings activate neutrophils via formyl peptide receptors and P44/42 MAP kinase. *J Orthop Trauma* **24**, 534-538.
20. Maeda, A., and Fadeel, B. (2014) Mitochondria released by cells undergoing TNF- α -induced necroptosis act as danger signals. *Cell Death Dis* **5**, e1312.
21. Hu, Q., Wood, C. R., Cimen, S., Venkatachalam, A. B., and Alwayn, I. P. J. (2015) Mitochondrial damage-associated molecular patterns (MTDs) are released during hepatic ischemia reperfusion and induce inflammatory responses. *PLoS One* **10**, e0140105.
22. Weinberg, S. E., Sena L. A., and Chandel, N. (2015) Mitochondria in the regulation of innate and adaptive immunity. *Immunity* **42**, 406-417.
23. Grazioli, S., and Pugin, J. N. (2018) Mitochondrial damage-associated molecular patterns: from inflammatory signaling to human diseases. *Front Immunol* **9**, 832.
24. Nakahira, K., Kyung, S. Y., Rogers, A. J., Gazourian, L., Youn, S., Massaro, A. F., Quintana, C., Osorio, J. C., Wang, Z., Zhao, Y., Lawler, L. A., Christie, J. D., Meyer, N. J., Mc Causland, F. R., Waikar, S. S., Waxman, A. B., Chung, R. T., Bueno, R., Rosas, I. O., Fredenburgh, L. E., Baron, R. M., Christiani, D. C., Hunninghake, G. M., and Choi, A. M. (2013) Circulating mitochondrial DNA in patients in the ICU as a marker of mortality: derivation and validation. *PLoS Med* **10**, e1001577.
25. Unuma, K., Aki, T., Matsuda, S., Funakoshi, T., Yoshida, K., and Uemura, K. (2013) Elimination and active extrusion of liver mitochondrial proteins during lipopolysaccharide administration in rat. *Hepato Res* **43**, 526-534.
26. Zhang, L., Deng, S., Zhao, S., Ai, Y., Zhang, L., Pan, P., Su, X., Tan, H., and Wu, D. (2016) Intra-Peritoneal Administration of mitochondrial DNA provokes acute lung injury and systemic inflammation via toll-like receptor 9. *Int J Mol Sci* **17**, E1425.
27. Deng, S. Y., Zhang, L. M., Ai, Y. H., Pan, P. H., Zhao, S. P., Su, X. L., Wu, D. D., Tan, H. Y., Zhang, L. N., and Tsung, A. (2017) Role of interferon regulatory factor-1 in lipopolysaccharide-induced mitochondrial damage and oxidative stress responses in macrophages. *Int J Mol Med* **40**, 1261-1269.

28. Podlesniy, P., Figueiro-Silva, J., Llado, A., Antonell, A., Sanchez-Valle, R., Alcolea, D., Lleo, A., Molinuevo, J. L., Serra, N., and Trullas, R. (2013) Low cerebrospinal fluid concentration of mitochondrial DNA in preclinical Alzheimer disease. *Ann Neurol* **74**, 655-668.
29. Wilkins, H. M., Weidling, I. W., Ji, Y., and Swerdlow, R. H. (2017) Mitochondria-derived damage-associated molecular patterns in neurodegeneration. *Front Immunol* **26**, 508.
30. Hazeldine, J., Hampson, P., Opoku, F. A., Foster, M., and Lord, J. M. (2015) N-Formyl peptides drive mitochondrial damage associated molecular pattern induced neutrophil activation through ERK1/2 and P38 MAP kinase signalling pathways. *Injury* **46**, 975-984.
31. Murphy, E., Ardehali, H., Balaban, R. S., DiLisa, F., Dorn, G. W. 2nd, Kitsis, R. N., Otsu, K., Ping, P., Rizzuto, R., Sack, M. N., Wallace, D., and Youle, R. J. (2016) Mitochondrial Function, Biology, and Role in Disease: A Scientific Statement From the American Heart Association. *Circ Res* **118**, 1960-1991.
32. Zhang, B., Asadi, S., Weng, Z., Sismanopoulos, N., and Theoharides, T. C. (2012) Stimulated human mast cells secrete mitochondrial components that have autocrine and paracrine inflammatory actions. *PLoS One* **7**, e49767.
33. Prikhodko, A. S., Shabanov, A. K., Zinovkina, L. A., Popova, E. N., Aznauryan, M. A., Lanina, N. O., Vitushkina, M. V., and Zinovkin, R. A. (2015) Pure Mitochondrial DNA Does Not Activate Human Neutrophils in vitro. *Biochemistry (Mosc)* **80**, 629-635.
34. Boulay, F., Tardif, M., Brouchon, L., and Vignais, P. (1990) Synthesis and use of a novel N-formyl peptide derivative to isolate a human N-formyl peptide receptor cDNA. *Biochem Biophys Res Commun* **168**, 1103-1109.
35. Quehenberger, O., Prossnitz, E. R., Cavanagh, S. L., Cochrane, C. G., and Ye, R. D. (1993) Multiple domains of the N-formyl peptide receptor are required for high-affinity ligand binding. Construction and analysis of chimeric N-formyl

- peptide receptors. *J Biol Chem* **268**, 18167-18175.
36. Murphy, P. M. (1994) The molecular biology of leukocyte chemoattractant receptors. *Annu Rev Immunol* **12**, 593-633.
 37. Seki, T., Fukamizu, A., Kiso, Y., and Mukai, H. (2011) Mitocryptide-2, a neutrophil-activating cryptide, is a specific endogenous agonist for formyl-peptide receptor-like 1. *Biochem Biophys Res Commun* **404**, 482-487.
 38. Dahlgren, C., Gabl, M., Holdfeldt, A., Winther, M., and Forsman, H. (2016) Basic characteristics of the neutrophil receptors that recognize formylated peptides, a danger-associated molecular pattern generated by bacteria and mitochondria. *Biochem Pharmacol* **114**, 22-39.
 39. Weiß, E., and Kretschmer, D. (2018) Formyl-peptide receptors in infection, inflammation, and cancer. *Trends Immunol* **39**, 815-829.
 40. Walker, J. E., Carroll, J., Altman, M. C., and Fearnley, I. M. (2009) Mass spectrometric characterization of the thirteen subunits of bovine respiratory complexes that are encoded in mitochondrial DNA. *Methods Enzymol* **456**, 111-131.
 41. Ott, M., Amunts, A., and Brown, A. (2016) Organization and regulation of mitochondrial protein synthesis. *Annu Rev Biochem* **85**, 77-101.
 42. Merrifield, R. B. (1963) Solid phase peptide synthesis. I. The synthesis of a tetrapeptide. *J Am Chem Soc* **85**, 2149-2154.
 43. Mukai, H., Kawai, K., Suzuki, Y., Yamashita, K., and Munekata, E. (1987) Stimulation of dog gastropancreatic hormone release by neuromedin B and its analogues. *Am J Physiol* **252**, E765-E771.
 44. Mukai, H., Munekata, E., and Higashijima, T. (1992) G protein antagonist. A novel hydrophobic peptide competes with receptor for G protein binding. *J Biol Chem* **267**, 16237-16243.
 45. Mukai, H., Kikuchi, M., Suzuki, Y., and Munekata, E. (2007) A mastoparan analog without lytic effects and its stimulatory mechanisms in mast cells. *Biochem Biophys Res Commun* **362**, 51-55.

46. Chaplinski, T. J., and Niedel, J. E. (1982) Cyclic nucleotide-induced maturation of human promyelocytic leukemia cells. *J Clin Invest* **70**, 953–964.
47. Nakajima, T., Wakamatsu, K., and Mukai, H. (2000) Mastoparan as a G protein-activator. *Methods and Tools in Biosciences and Medicine: Animal Toxins*. Birkhauser: Basel, Switzerland, 116-126.
48. Lind, S., Gabl, M., Holdfeldt, A., Mårtensson, J., Sundqvist, M., Nishino, K., Dahlgren, C., Mukai, H., and Forsman, H. (2019) Identification of residues critical for FPR2 activation by the cryptic peptide mitocryptide-2 originating from the mitochondrial DNA-encoded cytochrome b. *J Immunol* **202**, 2710-2719.
49. Offermanns, S., and Simon, M. I. (1995) Gα15 and Gα16 couple a wide variety of receptors to phospholipase C. *J Biol Chem* **270**, 15175-15180.
50. Williams, L. T., Snyderman, R., Pike, M. C., and Lefkowitz, R. J. (1977) Specific receptor sites for chemotactic peptides on human polymorphonuclear leukocytes. *Proc Natl Acad Sci USA* **74**, 1204-1208.
51. Niedel, J., Kahane, I., Lachman, L., and Cuatrecasas, P. (1980) A subpopulation of cultured human promyelocytic leukemia cells (HL-60) displays the formyl peptide chemotactic receptor. *Proc Natl Acad Sci USA* **77**, 1000-1004.
52. Krautwurst, D., Seifert, R., Hescheler, J., and Schultz, G. (1992) Formyl peptides and ATP stimulate Ca²⁺ and Na⁺ inward currents through non-selective cation channels via G-proteins in dibutyl cyclic AMP-differentiated HL-60 cells. Involvement of Ca²⁺ and Na⁺ in the activation of β-glucuronidase release and superoxide production. *Biochem J* **288**, 1025-1035.
53. Gysin, B., and Schwyzer, R. (1984) Hydrophobic and electrostatic interactions between adrenocorticotropin-(1-24)-tetracosapeptide and lipid vesicles. amphiphilic primary structures. *Biochemistry* **23**, 1811-1818.
54. Sargent, D. F., and Schwyzer, R. (1986) Membrane lipid phase as catalyst for peptide-receptor interactions. *Proc Natl Acad Sci USA* **83**, 5774-5778.
55. Zhuang, Y., Liu, H., Edward Zhou, X., Verma, K. R., de Waal, P. W., Jang, W., Xu, T.

- H., Wang, L., Meng, X., Zhao, G., Kang, Y., Melcher, K., Fan, H., Lambert, N. A., Eric Xu, H., and Zang, C. (2020) Structure of formylpeptide receptor 2-G_i complex reveals insights into ligand recognition and signaling. *Nat Commun* **11**, 885.
56. Wenceslau, C. F., McCarthy, C. G., Szasz, T., Goulopoulou, S., Webb, R. C. (2015) Mitochondrial N-formyl peptides induce cardiovascular collapse and sepsis-like syndrome. *Am J Physiol Heart Circ Physiol* **308**, H768-H777.
57. Dufton, N., Hannon, R., Brancaleone, V., Dalli, J., Patel, H. B., Gray, M., D'Acquisto, F., Buckingham, J. C., Perretti, M., Flower, R. J. (2010) Anti-inflammatory role of the murine formyl-peptide receptor 2: ligand-specific effects on leukocyte responses and experimental inflammation. *J Immunol* **184**, 2611-2619.
58. Kim, S. D., Kim, Y. K., Lee, H. Y., Kim, Y. S., Jeon, S. G., Baek, S. H., Song, D. K., Ryu, S. H., and Bae, Y. S. (2010) The agonists of formyl peptide receptors prevent development of severe sepsis after microbial infection. *J Immunol* **185**, 4302-4310.
59. Kim, S. D., Kwon, S., Lee, S. K., Kook, M., Lee, H. Y., Song, K. D., Lee, H. K., Baek, S. H., Park, C. B., and Bae, Y. S. (2013) The immune-stimulating peptide WKYMVm has therapeutic effects against ulcerative colitis. *Exp Mol Med* **45**, e40.
60. Kim, Y. E., Park, W. S., Ahn, S. Y., Sung, D. K., Sung, S. I., Kim, J. H., and Chang, Y. S. (2019) WKYMVm hexapeptide, a strong formyl peptide receptor 2 agonist, attenuates hyperoxia-induced lung injuries in newborn mice. *Sci Rep* **9**, 6815.
61. Babbitt, B. A., Jesaitis, A. J., Ivanov, A. I., Kelly, D., Laukoetter, M., Nava, P., Parkos, C. A., and Nusrat, A. (2007) Formyl peptide receptor-1 activation enhances intestinal epithelial cell restitution through phosphatidylinositol 3-kinase-dependent activation of Rac1 and Cdc42. *J Immunol* **179**, 8112-8121.
62. Zhang, X. G., Hui, Y. N., Huang, X. F., Du, H. J., Zhou, J., and Ma, J. X. (2011) Activation of formyl peptide receptor-1 enhances restitution of human retinal pigment epithelial cell monolayer under electric fields. *Invest Ophthalmol Vis Sci* **52**, 3160-3165.

63. Shao, G., Julian, M. W., Bao, S., McCullers, M. K., Lai, J. P., Knoell, D. L., and Crouser, E. D. (2011) Formyl peptide receptor ligands promote wound closure in lung epithelial cells. *Am J Respir Cell Mol Biol* **44**, 264-269.
64. Liu, M., Chen, K., Yoshimura, T., Liu, Y., Gong, W., Le, Y., Gao, J. L., Zhao, J., Wang, J. M., Wang, A. (2014) Formylpeptide receptors mediate rapid neutrophil mobilization to accelerate wound healing. *PLoS One* **9**, e90613.
65. Zhang, L., Wang, H., Yang, T., Su, Z., Fang, D., Wang, Y., Fang, J., Hou, X., Le, Y., Chen, K., Wang, J. M., Su, S. B., Lin, Q., and Zhou, Q. (2015) Formylpeptide receptor 1 mediates the tumorigenicity of human hepatocellular carcinoma cells. *Oncoimmunology* **5**, e1078055.
66. Gabl, M., Sundqvist, M., Holdfeldt, A., Lind, S., Mårtensson, J., Christenson, K., Marutani, T., Dahlgren, C., Mukai, H., and Forsman, H. (2018) Mitocryptides from Human Mitochondrial DNA–Encoded Proteins Activate Neutrophil Formyl Peptide Receptors: Receptor Preference and Signaling Properties. *J Immunol* **200**, 3269-3282.
67. Mukai, H., Ueki, N., Wakamatsu, K., and Kiso, Y. (2009) Cryptide signal: a novel signaling mechanisms involving cryptides. *Peptides (Proceedings of European Peptide Symposium)* **2008**, 570-571.
68. Hattori, T., and Mukai, H. (2014) クリプタイドタンパク質に隠された新しい生理活性ペプチド。 *日本薬理学雑誌* **144**, 234-238.
69. Hattori, T., Nakashima, K., Marutani, T., Kiso, Y., Nishi, Y., Mukai, H. (2015) Successful acquisition of a neutralizing monoclonal antibody against a novel neutrophil-activating peptide, mitocryptide-1. *Biochem Biophys Res Commun* **463**, 54-59.
70. Hattori, T., Yamada, T., Morikawa, H., Marutani, T., Tsutsumi, K., Nishino, K., Shimizu, T., Nishi, Y., Kiso, Y., Mukai, H. (2017) Generation of monoclonal antibodies against mitocryptide-2: Toward a new strategy to investigate the biological roles of cryptides. *J Pept Sci* **23**, 610-617.

71. Marutani, T., Nakashima, K., Tsutsumi, K., Hattori, T., Nishino, K., Shimizu, T., Kiso, Y., and Mukai, H. (2016) Mitocryptide-3: Characterization of its receptor molecules. *Peptide Science (Proceedings of Japanese Peptide Symposium)* **2015**, 251–252.
72. Marutani, T., Tamura, S., Nakashima, K., Nishino, K., Morikawa, H., Hattori, T., Kiso, Y., and Mukai, H. (2018) Investigation of signaling mechanisms induced by mitocryptide-3, a novel neutrophil-activating peptide derived from a mitochondrial transit sequence. *Peptide Science (Proceedings of Japanese Peptide Symposium)* **2017**, 138–139.
73. Marutani, T., Tamura, S., Nakashima, K., Nishino, K., Morikawa, H., Hattori, T., Kiso Y, and Mukai, H. (2019) Mitocryptide-3: Investigation of Signaling Mechanisms Induced by a Novel Neutrophil-Activating Peptide Derived from a Mitochondrial Transit Sequence. *Peptide Science (Proceedings of Japanese Peptide Symposium)* **2018**, 34.
74. Ohura, K., Marutani, T., Tamura, S., Nakashima, K., Morikawa, H., Kiso Y, and Mukai, H. (2021) Recognition Mechanisms of Mitocryptide-2 by Formy-Peptide Receptor 2. *Peptide Science (Proceedings of Japanese Peptide Symposium)* **2020**, 99–100.
75. Marutani, T., Kiso, Y., and Mukai, H. (2019) 創薬を目指した生理活性ペプチド研究の新展開～クリプタイトドを中心として～. ペプチド創薬の最前線 (シーエムシー出版) 247-257.

List of publications

1. Marutani, T., Hattori, T., Koike, Y., Harada, A., Watanabe, K., Kiso, Y., and Mukai, H. (2014) Endogenous N-formylated cryptides: Investigation of their biological functions. *Peptide Science* **2013**, 249-250.
2. Hattori, T., Nakashima, K., Marutani, T., Kiso, Y., Nishi, Y., Mukai, H. (2015) Successful acquisition of a neutralizing monoclonal antibody against a novel neutrophil-activating peptide, mitocryptide-1. *Biochem Biophys Res Commun* **463**, 54-59.
3. Marutani, T., Hattori, T., Koike, Y., Harada, A., Watanabe, K., Kiso, Y., and Mukai, H. (2015) Mitocryptide-2: Structure-Activity Relationships for the Elucidation of Ligand Recognition Mechanisms of Formyl-Peptide Receptor Like. *Peptides* **2014**, 6-8.
4. Marutani, T., Hattori, T., Tsutsumi, K., Koike, Y., Harada, A., Noguchi, K., Kiso, Y., Mukai, H. (2016) Mitochondrial protein-derived cryptides: are endogenous N-formylated peptides including mitocryptide-2 components of mitochondrial damage-associated molecular patterns?. *Biopolymers (Pept Sci)* **106**, 580-587.
5. Marutani, T., Nakashima, K., Tsutsumi, K., Hattori, T., Nishino, K., Shimizu, T., Kiso, Y., and Mukai, H. (2016) Mitocryptide-3: Characterization of its receptor molecules. *Peptide Science* **2015**, 251-252.
6. Nishino, K., Marutani, T., Tsutsumi, K., Hattori, T., Kiso, Y., and Mukai, H. (2017) Structure-Activity Relationships of Mitocryptide-2 for the Elucidation of Ligand Recognition Mechanisms of Formyl-Peptide Receptor 2. *Peptide Science* **2016**,

107-108.

7. Hattori, T., Yamada, T., Morikawa, H., Marutani, T., Tsutsumi, K., Nishino, K., Shimizu, T., Nishi, Y., Kiso, Y., Mukai, H. (2017) Generation of monoclonal antibodies against mitocryptide-2: Toward a new strategy to investigate the biological roles of cryptides. *J Pept Sci* **23**, 610-617.
8. Shimizu, T., Hattori, T., Marutani, T., Kiso, Y., and Mukai, H. (2018) Possible Existence of *N*-Formylated Peptides Derived from Cytochrome c Oxidase Subunit I. *Peptide Science* **2017**, 74-75.
9. Nishino, K., Marutani, T., Hattori, T., Kiso, Y., and Mukai, H. (2018) Mitocryptide-2: Ligand Recognition Mechanisms of Formyl-Peptide Receptor 1 and Its Homologue Formyl-Peptide Receptor 2. *Peptide Science* **2017**, 114-115.
10. Marutani, T., Tamura, S., Nakashima, K., Nishino, K., Morikawa, H., Hattori, T., Kiso, Y., and Mukai, H. (2018) Investigation of signaling mechanisms induced by mitocryptide-3, a novel neutrophil-activating peptide derived from a mitochondrial transit sequence. *Peptide Science* **2017**, 138-139.
11. Gabl, M., Sundqvist, M., Holdfeldt, A., Lind, S., Mårtensson, J., Christenson, K., Marutani, T., Dahlgren, C., Mukai, H., and Forsman, H. (2018) Mitocryptides from Human Mitochondrial DNA-Encoded Proteins Activate Neutrophil Formyl Peptide Receptors: Receptor Preference and Signaling Properties. *J Immunol* **200**, 3269-3282.
12. Marutani, T., Tamura, S., Nakashima, K., Nishino, K., Morikawa, H., Hattori, T., Kiso Y, and Mukai, H. (2019) Mitocryptide-3: Investigation of Signaling

Mechanisms Induced by a Novel Neutrophil-Activating Peptide Derived from a Mitochondrial Transit Sequence. *Peptide Science* **2018**, 34.

13. 丸谷飛之, 木曾良明, 向井秀仁. (2019) 創薬を目指した生理活性ペプチド研究の新展開〜クリプトイドを中心として〜. *ペプチド創薬の最前線* (シーエムシー出版) 247-257.
14. Sugimoto, Y., Morikawa, H., Ojima, T., Marutani, T., Kiso Y, and Mukai, H. (2021) Mitocryptides: Presence and Molecular Forms in Mitochondrial Damage Associated Molecular Patterns. *Peptide Science* **2020**, 39-40.
15. Kamada, K., Marutani, T., Nishino, K., Ohura, K., Kiso Y, and Mukai, H. (2021) Recognition Mechanisms of Mitocryptide-2 by Formy-Peptide Receptor 2. *Peptide Science* **2020**, 75-76.
16. Ohura, K., Marutani, T., Tamura, S., Nakashima, K., Morikawa, H., Kiso Y, and Mukai, H. (2021) Recognition Mechanisms of Mitocryptide-2 by Formy-Peptide Receptor 2. *Peptide Science* **2020**, 99-100.
17. Marutani, T., Nishino, K., Miyaji, T., Kamada, K., Ohura, K., Kiso, Y., and Mukai, H. (2021) Mitocryptide-2: Identification of Its Minimum Structure for Specific Activation of FPR2–Possible Receptor Switching from FPR2 to FPR1 by Its Physiological C-terminal Cleavages. *Int J Mol Sci* **22**, 4084.